Your Interlibrary Loan request has been sent by email in a PDF format.

If this PDF arrives with an incorrect OCLC status, please contact lending located below.

Concerning Copyright Restrictions

FSU Faculty and Staff: Please refer to Copyright Resources Research Guide for additional information at http://guides.lib.fsu.edu/copyright

Interlibrary Loan Services: We Search the World for You…and Deliver!

Interlibrary Loan Services – FSU Community
Florida State University
R.M. Strozier Library
116 Honors Way
Tallahassee, Florida 32306-2047
Email: lib-borrowing@fsu.edu
Website: https://www.lib.fsu.edu/find-and-borrow/extended-borrowing
Phone: 850.644.4466

Non-FSU Institutions:
Email: lib-lending@fsu.edu
Phone: 850.644.4466

Rapid #: -25175154

CROSS REF ID: **1105810**

LENDER: **NJP (William Paterson University of New Jersey) :: Cheng Library**

BORROWER: **FDA (Florida State University) :: Main Library**

TYPE:	Article CC:CCG
JOURNAL TITLE:	Marine chemistry
USER JOURNAL TITLE:	Marine Chemistry
ARTICLE TITLE:	Unsaturated aliphatic and sulfur-containing organic matter as surfactants in the surface microlayer
ARTICLE AUTHOR:	N.R. Coffey, F.E. Agblemanyo, A.M. McKenna, A.S. W
VOLUME:	272
ISSUE:	
MONTH:	9
YEAR:	2025
PAGES:	104547
ISSN:	0304-4203
OCLC #:	

Processed by RapidX: 9/8/2025 4:42:06 PM

Marine Chemistry 272 (2025) 104547

Contents lists available at ScienceDirect

Marine Chemistry

journal homepage: www.elsevier.com/locate/marchem

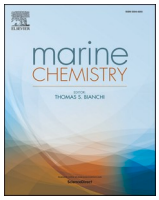

Unsaturated aliphatic and sulfur-containing organic matter as surfactants in the surface microlayer

N.R. Coffey [a,b,*], F.E. Agblemanyo [a], A.M. McKenna [c,d], A.S. Wozniak [a,**]

[a] School of Marine Science and Policy, University of Delaware, Lewes, DE 19958, USA
[b] Department of Earth and Environmental Sciences, University of Minnesota, Minneapolis, MN 55455, USA
[c] National High Magnetic Field Laboratory, Florida State University, Tallahassee, FL 32310, USA
[d] Department of Soil and Crop Sciences, Colorado State University, Fort Collins, CO 80523, USA

ARTICLE INFO

Keywords:
Surface microlayer
FT-ICR MS
Unsaturated aliphatic compounds
Organic sulfur

ABSTRACT

The surface microlayer (SML) is a 10s–100s μm thick layer which mediates fluxes across the air-sea interface. Organic matter (OM) enrichments at the SML are known to influence SML physical properties and air-sea exchanges, but the role of detailed molecular level OM composition in influencing those processes hasn't been fully explored. SML and subsurface (SUB, 8–15 cm) water at four stations encompassing different influences (marine/fluvial/salt marsh) on the Delaware Bay system were sampled and examined for relationships between SML/SUB OM composition and surface tension. Samples collected December 2018–October 2019 show SML dissolved organic carbon (DOC) enrichments of 0.87 to 4.42 times the SUB concentration. Excitation-emission matrix spectroscopy (EEMs) and negative electrospray ionization (-ESI) Fourier-transform ion cyclotron resonance mass spectrometry (FT-ICR MS) show marine samples have higher contributions from photobleached material and higher relative abundances of CHON compounds relative to inner bay sites, respectively. Principal component analyses further reveal consistent differences in SML OM composition relative to SUB. The SML contains higher abundances of compounds with H/C > 1.7 and O/C < 0.2, including sulfur-containing compounds - compositions suggestive of surfactant-like molecules, able to depress surface tension at the air-sea interface. Surface tension depressions were significantly correlated with unsaturated aliphatic and sulfur-containing compounds identified from FT-ICR MS data, yet showed no relationship with DOC abundances or enrichments, highlighting the need for compositional assessments for understanding OM influences on SML properties and air-sea exchanges. The sources and structures of SML surfactant molecules should be a focus of future work.

1. Introduction

The surface microlayer (SML) is the 10s–100s μm thick layer at the air-water interface of bodies of water known to possess distinct biological, chemical, and physical characteristics relative to the underlying water. Because of its unique position between air and the water column, the SML influences materials exchanged across that interface (Jenkinson et al., 2018). The SML's impact on these exchanges is often attributed to enrichments of organic matter (OM) and surfactant activity (e.g., Rickard et al., 2022; Sabbaghzadeh et al., 2017; Wurl et al., 2011). Due to their amphiphilic properties, surfactants in underlying waters are attracted to bubble surfaces and subsequently transported to the SML, where they accumulate creating a distinct organic molecular microenvironment. High exposure to UV light in the SML facilitates photochemical transformation which alters the properties of accumulated surfactants, further altering the SML's organic composition and physical properties relative to subsurface waters (e.g., Blough, 1997; Galgani and Engel, 2016; Miranda et al., 2018; Rickard et al., 2022). These surfactants are important constituents of primary marine aerosols ejected into the atmosphere with breaking waves (e.g., Frossard et al., 2019; Lewis and Schwartz, 2004) and thus impact the production, composition, and climate-relevant properties of primary marine aerosols emitted from the sea surface (Gantt and Meskhidze, 2013; Wilson et al., 2015). SML surfactants also serve to reduce surface tension, as well as reduce gas

* Correspondence to: NR Coffey, 241 Amundson Hall, 421 Washington Ave. SE, Minneapolis, MN 55455, USA.
** Correspondence to: AS Wozniak, 210 Cannon Lab, 1044 College Drive, Lewes, DE 19958, USA.
E-mail addresses: coffe198@umn.edu (N.R. Coffey), fedufia@udel.edu (F.E. Agblemanyo), mckenna@magnet.fsu.edu (A.M. McKenna), awozniak@udel.edu (A.S. Wozniak).

https://doi.org/10.1016/j.marchem.2025.104547
Received 12 March 2025; Received in revised form 10 July 2025; Accepted 18 July 2025
Available online 20 July 2025

transfer coefficients and gas exchange rates across the air-sea interface (e.g., Frew et al., 2006; Frew et al., 1990; Goldman et al., 1988; Mustaffa et al., 2020; Pereira et al., 2018). The exchanges of gases such as O_2, CO_2, N_2O, dimethylsulfide, and volatile organic compounds (VOCs), for example, across the air-sea interface are of particular interest due to their implications for biological activity, carbon cycling, and climate change (Carpenter et al., 2012; Wurl et al., 2016). The reduced surface tension in the SML also influences dry deposition of particles to the water column, slowing particle settling speeds (Del Vento and Dachs, 2007). Given the importance of surfactant OM on physical properties and material exchanges at the air-sea interface, the identities and sources of the surfactant OM compounds, as well as the processes that govern their variations, warrant thorough investigation.

SML enrichments have been widely observed for the total, dissolved, and particulate OM pools (e.g., Carlson, 1983; Frew et al., 2006; Huang et al., 2015; Marty et al., 1988). However, not all components of these enriched pools of OM influence SML physical properties equivalently, as demonstrated by laboratory experiments using model compounds (Goldman et al., 1988; Siddiqui and Franses, 1996). The differential impacts of surfactants on surface tension and viscoelasticity result from differences in molecular features such as hydrophobic alkyl chain lengths and hydrophilic functional group structure and ionicity (Frew, 1997; Zhang and Marchant, 1996). Thus, an understanding of the molecular identities of seawater surfactants, and processes governing their transformations within the SML, are important for understanding their impacts.

Amphiphilic, surfactant-like compounds have justifiably been a major focus of SML studies due to their presumed attraction to bubbles and the air-water interface and impact on surface tension and air-sea exchanges (Burdette et al., 2022; Frew et al., 2006; Marty et al., 1988; Wurl et al., 2011). Various classes of biologically-derived compounds (e.g., fatty acids, phospholipid fatty acids, amino acids, polysaccharides, wax esters, glycerides, and other lipids; e.g., Brinis et al., 2004; Engel and Galgani, 2016; Frew et al., 2006; Myklestad, 1974; Nichols and Espey, 1991; Penezić et al., 2022; Sakugawa and Handa, 1985; Tilstone et al., 2010; Zäncker et al., 2017) fit this description and have been shown to be more enriched than the bulk organic carbon pool, though enrichments vary in time and space. Such work underscores the influence of biology on the SML. Microbiological data suggest that the SML supports plentiful bacterial populations that are distinct from that of subsurface waters (Cunliffe et al., 2011). While the focus on quantifiable biomarker compounds has been fruitful for demonstrating a likely biological influence on SML surfactant activity, there is a need for untargeted molecular characterization of SML organics to identify surface tension reducing components. The DOM pool is extremely diverse, and has been demonstrated to contain tens to hundreds of thousands of compounds (Kim et al., 2003; Moran et al., 2016). Microorganisms release a diverse pool of metabolites (Bercovici et al., 2022; Longnecker et al., 2015), significantly contributing to the DOM pool. The extensive suite of biologically-produced compounds may be rapidly degraded in the environment, through both abiotic (e.g., photodegradation, Bittar et al., 2015b, Bittar et al., 2015a) and biological processes (Bittar et al., 2015b; Kujawinski, 2011). Both photodegradation and biological activity are amplified at the SML, where solar irradiation is highest and biological communities are enriched. Many of these degradation products are unidentified, necessitating untargeted analyses to assess this suite of potential surfactant compounds.

Non-targeted mass spectrometric studies of the SML reveal it to be enriched in molecules with low O/C and high H/C ratios (Burdette et al., 2022; Frew et al., 2006; Lechtenfeld et al., 2013) and that contain sulfur (Lechtenfeld et al., 2013). Such molecules fit within the scope of the amphiphilic surfactant-like molecules. Correlating molecular-level speciation with measurements of physical properties (e.g., surface tension) can provide invaluable insight into relevant physicochemical relationships. For example, Frew et al. (2006) found a strong correlation between elasticity and a discriminant variable characterized by contributions from fatty acids, bound acyl lipids, wax esters, glycerides, and sterols identified by desorption ionization mass spectrometry. Notably, advances in mass spectrometric approaches (including electrospray ionization 9.4 T Fourier transform ion cyclotron resonance mass spectrometry (FT-ICR MS) and related techniques allow for characterization of a much broader swath of the DOM pool.

Untargeted spectroscopic characterization of the fluorophoric (FDOM) and chromophoric (CDOM) dissolved organic matter in the SML reveal enrichments of FDOM (Mustaffa et al., 2018; Mustaffa et al., 2017) and CDOM (Frew et al., 2004; Galgani and Engel, 2016; Tilstone et al., 2010; Zäncker et al., 2017), and indicate elevated influence from biological activity (e.g., Galgani and Engel, 2016) relative to the underlying water. While CDOM and FDOM are valuable for assessing DOM source and processing at relatively low cost and effort, the technique characterizes only the portion of the DOM pool that contains chromophoric and fluorophoric conjugated double bond systems (D'Andrilli et al., 2022; Leresche et al., 2022). Surfactant activity is expected to be higher for compounds containing hydrophobic alkyl chains not characterized with these techniques (Frew, 1997), necessitating additional techniques for characterizing SML surfactants. Nonetheless, the DOM source and process information obtained with CDOM and FDOM techniques pairs well with mass spectrometric approaches.

In this study, we combine data on bulk OM quantification, molecular-level OM characterization by 9.4 T FT-ICR mass spectrometry, and optical spectroscopic characteristics with surface tension measurements to identify organic matter constituents that could be influencing SML physical properties. SML and subsurface (SUB) waters were sampled seasonally at four locations throughout Delaware Bay in order to capture variations in properties (e.g., biological influence, relative terrestrial vs. marine influence, temperature, solar irradiance) expected to influence SML and SUB organic composition. Our results indicate that unsaturated aliphatic molecules and compounds containing sulfur are associated with surface tension depression in the SML, highlighting the importance of molecular-level characterization of the SML in assessing and predicting SML physical properties as well as identifying a suite of molecular classes of interest for future SML surfactant studies.

2. Methods

2.1. Sample collection, handling, and storage

2.1.1. Site selection

The Delaware Bay is a dynamic tidal system, influenced by both the marine environment through its connection to the Atlantic Ocean as well as freshwater inputs. The system is characterized by a variety of landscapes and land uses, including wetlands, agriculture, sewage treatment facilities, and human development, which influence its biogeochemistry. Four sites were selected throughout the Delaware Bay area to capture some of this variability in watershed influence as well as physicochemical properties (e.g., depth, salinity; Fig. 1, Table 1). This environmental variability was expected to result in concurrent variations in OM molecular composition and SML properties including surface tension.

The four sampling sites encompass different micro-environments found within the bay. The marine-influenced station, located just outside of the bay mouth, has the highest salinity and captures oceanic influences on Delaware Bay's SML. The mid-bay station is located within the main channel of the bay. Two estuarine sites at the mouths of the Murderkill and Broadkill Rivers where they meet Delaware Bay have higher relative terrestrial influence. The Murderkill watershed is dominated by agricultural land use (65 %), as well as forested areas and wetlands (30 %), and the sample site is downstream of a water treatment plant (http://delawarewatersheds.org/the-delaware-bay-estuary-basin/murderkill-river/, last accessed 05 August 2020). The Broadkill watershed is primarily composed of agricultural land (50 %) and

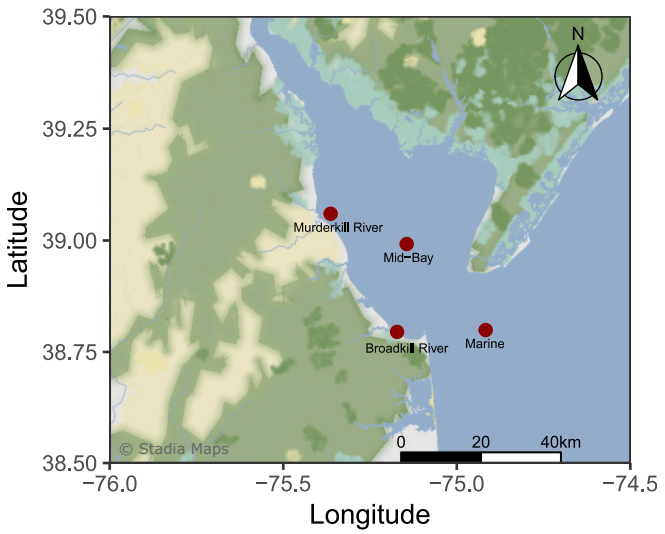

Fig. 1. Map of this study's sampling locations within Delaware Bay. Figure generated using Stadia Maps (stadiamaps.com) and Stamen Design (stamen.com).

wildlife refuges with extensive wetlands (http://delawarewatersheds.org/the-delaware-bay-estuary-basin/broadkill-river/, last accessed 05 August 2020). Cordgrass (*Spartina alterniflora*)-dominated wetlands line both the Murderkill and Broadkill estuaries near their mouths.

2.1.2. Sampling and sample processing

Samples of SML and SUB water were collected aboard R/V Joanne Daiber. The marine and mid-bay stations were sampled in December 2018, and all stations were sampled in March, June, August, and October of 2019. Sampling at each site was performed upwind of the engines with the engines and generator turned off to avoid contamination from the vessel. SML samples were collected at a distance of approximately 1–2 m from the vessel using a modified glass plate sampler attached to a Teflon-wrapped PVC pole, following previously established methods (Cunliffe et al., 2009; Harvey, 1966; Harvey and Burzell, 1972; Jun et al., 1998). Briefly, the glass plate sampler was inserted into the water perpendicular to the water's surface, and slowly withdrawn at a rate of ~20 cm/s. The sampler was allowed to drip freely for 10 s to remove subsurface water contamination, and then the sample was transferred into an acid-cleaned polycarbonate bottle using a PTFE squeegee and an acid-cleaned, pre-combusted (450 °C, 6 h) glass funnel. SUB samples were collected directly into an acid-cleaned polycarbonate bottle. Field measurements of pH, salinity, water temperature, and water depth were recorded on site. A field blank was obtained once per sampling excursion by collecting ultrapure water (DOC below detection limit) as it was poured over the cleaned sampler then squeegeed into the collection funnel and bottle.

Upon arrival at the laboratory, an aliquot of unfiltered sample was set aside for surface tension analysis. The remaining sample was filtered through 0.7 μm GF/F filters using a vacuum filtration setup into a clean glass Erlenmeyer flask. All glassware and filters were combusted at 450 °C for 6 h prior to use. The filters were placed in combusted foil pouches and frozen. The filtrate was collected into a clean polycarbonate sample bottle. Analyses were conducted within a week of sample collection whenever possible, and immediately frozen (−9 °C) if circumstances prevented immediate analysis.

2.2. POC analysis

Particulate samples on the frozen 0.7 μm GF/F filters were thawed and dried. Subsamples were collected using stainless steel punches. Samples were placed in a glass chamber and fumigated with hydrochloric acid fumes for 24 h to remove carbonates from the samples. Samples were then tinned for analysis. Carbon, nitrogen, and hydrogen were quantified using high temperature catalytic oxidation on a Costech ECS4010 CHNS Elemental Analyzer calibrated using an ethylenediaminetetraacetic acid standard curve.

2.3. DOC analyses

2.3.1. Quantification

Filtered samples were poured into 30 mL vials and acidified to a pH of 2 using 2 M HCl. Samples were analyzed using a Shimadzu TOC-V CPH Total Organic Carbon Analyzer operated at 680 °C, calibrated using a potassium hydrogen phthalate (LabChem) standard following previous work (Wozniak et al., 2012). Certified seawater reference standards (Hansell Laboratory, DSR Lot # 07–07, 41–45 μM DOC) were run with each set of samples to check for instrument drift. Concentrations calculated for field blanks were subtracted from those of their corresponding samples.

SML properties are often reported in relation to those of the corresponding SUB using the enrichment factor (EF, e.g., Chen et al., 2016; Dreshchinskii and Engel, 2017; Liss and Duce, 1997) as demonstrated for DOC using the following equation, where $[DOC]_{SML}$ is the concentration of DOC in the SML, and $[DOC]_{SUB}$ is the concentration of DOC in the SUB water (Eq. (1)):

$$EF_{DOC} = \frac{[DOC]_{SML}}{[DOC]_{SUB}} \quad (1)$$

EF >1 is evidence for DOC enrichment in the SML relative to SUB, while an EF < 1 demonstrates a depletion of DOC in the SML. Similar EF values can also be calculated for POC, as well as components of the DOC pool.

2.3.2. Optical measurements

The absorbance spectrum of CDOM was obtained between the wavelengths of 230 nm and 700 nm (2 nm resolution) using a Horiba Aqualog® with a pathlength of 1 cm. If the absorbance at λ = 254 nm was above 0.2, the sample was diluted to avoid saturating the fluorescence detector. Fluorescence excitation emission matrix spectroscopy (EEMs) was performed over an excitation/emission (ex/em) range of 230–700 nm/245–822 nm using a Horiba Aqualog® with an increment of 2 nm and an emission interval of 4.65 nm. Each EEM was subjected to an inner filter effect correction using absorbance data collected as described above (McKnight et al., 2001). Spectra were also blank corrected using an EEM generated from a field blank and Raman calibrated (Lawaetz and Stedmon, 2009). Spectra were normalized by the integrated fluorescent intensity of the sample to control for differences in concentration across the dataset. The humification index (HIX; Ohno, 2002) and biological index (BIX; Huguet et al., 2009) were calculated

Table 1
Locations and physicochemical properties of each sampling site at the time of sampling over the course of the study (December 2018 – October 2019).

Station	Latitude	Longitude	Salinity	Depth, m	pH
Marine	38° 47′ 57.3" N	74° 55′ 0.37" W	27–33	13.0–21.2	7.93–8.17
Mid-Bay	38° 59′ 31.81" N	75° 8′ 39.37" W	22–29	9.8–14.7	8.00–8.24
Murderkill River	39° 3′ 35.57" N	75° 21′ 48.35" W	16–27	2.4–4.2	7.93–8.11
Broadkill River	38° 47′ 42.25" N	75° 10′ 19.2" W	11–30.5	2.3–3.4	7.09–8.01

using the eemR package in R (Massicotte, 2019). Peaks known to represent terrestrial humic-like, marine humic-like, and protein-like fluorophores (Coble, 1996) were also identified using this R package, and a peak representing photobleached organic matter (Murphy et al., 2008) was quantified manually. A summary of these peaks of interest and indices including the excitation and emission wavelength ranges used to calculate them can be found in Table S1.

2.3.3. Electrospray Ionization 9.4 T Fourier transform ion cyclotron resonance mass spectrometry (FT-ICR MS)

2.3.3.1. Sample preparation. Dissolved samples were solid-phase extracted with PPL (Agilent Technologies) cartridges following standard methods (e.g., Dittmar et al., 2008; Mitra et al., 2013) for the purpose of concentrating the DOM and removing salts that interfere with electrospray ionization. PPL is known to retain the relatively hydrophobic portion of the DOM which has been found to account for 43–65 % of DOM (Dittmar et al., 2008), while more hydrophilic DOM is lost. Samples were eluted with 1.5–3 mL HPLC-grade methanol to obtain an estimated final concentration of ~50 mg C L^{-1}, assuming a 50 % recovery from the PPL cartridge.

2.3.3.2. Instrumentation

2.3.3.2.1. ESI source. As the surfactants of the SML are known to be mostly anionic in nature (Huang et al., 2015; Jaafar et al., 2014; Marty et al., 1988), all samples were run in negative electrospray ionization mode. Sample solution was infused via a microelectrospray source (Emmett et al., 1998; 50 μm i.d. fused silica emitter) at 500 nL/min by a syringe pump. Typical conditions for negative ion formation were: emitter voltage, −2.4-2.9 kV; tube lens, −250 V; and heated metal capillary current, 7 A.

2.3.3.2.2. 9.4 T FT-ICR MS. DOM extracts were analyzed with a custom-built hybrid linear ion trap FT-ICR mass spectrometer equipped with a 9.4 T superconducting solenoid magnet (Kaiser et al., 2011). Ions were initially accumulated in an external multipole ion guide (1–5 ms) and released *m/z*-dependently by decrease of an auxiliary radio frequency potential between the multipole rods and the end-cap electrode (Kaiser et al., 2014). Ions were excited to m/z-dependent radius to maximize the dynamic range and number of observed mass spectral peaks (32–64 %) (Kaiser et al., 2013), and excitation and detection were performed on the same pair of electrodes (Chen et al., 2014). The dynamically harmonized ICR cell in the 9.4 T FT-ICR MS is operated with 6 V trapping potential (Boldin and Nikolaev, 2011; Kaiser et al., 2011). Time-domain transients of 7.2 s were acquired with the Predator data station, with 100 time-domain acquisitions averaged for all experiments (Blakney et al., 2011). Mass spectra were internally calibrated with five high-abundance homologous series that span the sample molecular weight distribution based on the "walking" calibration method (Savory et al., 2011). Experimentally measured masses were converted from the International Union of Pure and Applied Chemistry (IUPAC) mass scale to the Kendrick mass scale (Kendrick, 1963) for rapid identification of homologous series for each heteroatom class (i.e., species with the same $C_cH_hN_nO_oS_s$ content, differing only by degree of alkylation; (Hughey et al., 2001). For each elemental composition, $C_cH_hN_nO_oS_s$, the heteroatom class, type (double bond equivalents, DBE = number of rings plus double bonds to carbon, $DBE = C - h/2 + n/2 + 1$; McLafferty and Turecek, 1993) and carbon number, *c*, were tabulated for subsequent generation of heteroatom class relative abundance distributions and graphical relative-abundance weighted images and van Krevelen diagrams. Peaks with signal magnitude greater than 6 times the baseline root-mean-square (RMS) noise at *m/z* 500 were internally calibrated, absorption-mode processed (Xian et al., 2010), and exported (Savory et al., 2011) to a peak list. Molecular formula assignments and data visualization were performed with PetroOrg © software (Corilo, 2014). Molecular formula assignments with an error > 0.5 ppm were discarded, and only chemical classes with a combined relative abundance of 0.15 % of the total were considered.

2.4. Surface tension measurements

Measurements of surface tension were collected using a Sigma 700 Tensiometer with a platinum ring (ring radius, $R = 0.9545$ cm; ring wire radius, $R' = 0.0185$ cm). Prior to each measurement, the ring was flame-sterilized to remove any traces of organic material that may have lingered on the wire. Unfiltered sample was allowed to come to room temperature, shaken to ensure the sample was homogenous, and then poured into a glass dish (diameter = 4.6 cm). This sample was allowed to stabilize for 10 min prior to data collection to ensure consistent measurements. The tensiometer obtained surface tension values by measuring the force required to break the surface of the sample by raising and lowering the ring at the air-water interface. Though the 10 min stabilization period is essential for reproducible measurements, this may allow surfactants to gather at the air-water interface and subsequently artificially lower measured surface tension compared to in-situ "true" values which cannot be measured directly. While this is a known limitation of this approach, surface tension measurements can still be expected to reflect to the differences in SML and SUB composition.

Surface tension depression in this study is defined as the lowering of surface tension in the SML relative to SUB. It was calculated by subtracting the surface tension of the SML sample from that of its paired SUB sample. A positive value for surface tension depression indicates that the microlayer has a lower surface tension than its paired SUB sample (Eq. (2)).

$$Surface\ Tension\ Depression = SUB\ Surface\ Tension - SML\ Surface\ Tension \quad (2)$$

Statistical Analyses

All data analyses were conducted in R version 4.2.1 (R Core Team, 2022). To assess normality, the Shapiro-Wilk test was applied to datasets with fewer than 5000 observations, while the Anderson-Darling test was used for larger datasets (FT-ICR molecular formulas) (Razali and Wah, 2011). Based on these results, appropriate parametric or non-parametric statistical tests were applied. The Wilcoxon rank sum test, and in some cases the *t*-test, was used to compare means between two sample groups. Spearman correlation analysis was conducted between organic matter measurements and surface tension depression to identify molecular and chemical properties potentially influencing surface tension. For FT-ICR MS data, only molecular formulas present in at least half of the samples were included in the analysis. Statistical significance was defined as $p < 0.05$.

Principal component analyses were performed using the "prcomp" function found in the base R package, "stats" (v4.2.1; R Core Team, 2022). Principal component analysis reduces many variables into fewer dimensions (called "principal components," PCs) via an orthogonal transformation. The relative abundances of each molecular formula identified by FT-ICR MS found across samples (n = 25,958) served as input data to the PCA. A PCA examining all samples was performed to evaluate the variance observed across spatial scales in the study dataset. PCAs were also run for each station individually to facilitate identification of SUB-SML differences within a given site.

3. Results

3.1. Bulk organic carbon concentrations and surface tension properties

The DOC and POC concentrations in SML samples ranged from 123.5 to 490.78 μM (median = 177.83 μM) and 24.53 to 476.76 μM (median =

Table 2
SML DOC and POC enrichments and surface tension depressions for all samples measured in this study.

Station	Sampling Date	EF_{DOC}	EF_{POC}	Surface Tension Depression, mN/m
Marine	4-Dec-18	4.42	0.66	–
	29-Mar-19	1.33	1.71	0.12
	12-Jun-19	1.44	1.27	0.45
	13-Jun-19	1.53	0.71	0.38
	14-Jun-19	1.67	1.22	0.14
	22-Aug-19	1.39	2.99	1.09
	1-Oct-19	1.27	1.44	0.31
Mid-Bay	4-Dec-18	1.23	1.04	–
	29-Mar-19	1.29	0.89	0.16
	12-Jun-19	1.18	1.04	0.46
	13-Jun-19	1.47	0.43	0.35
	14-Jun-19	1.12	–	0.08
	22-Aug-19	1.29	1.47	0.45
	1-Oct-19	1.24	1.26	0.35
Murderkill	29-Mar-19	0.87	2.41	1.01
	12-Jun-19	1.11	0.81	−0.08
	22-Aug-19	1.29	0.81	0.58
	1-Oct-19	1.64	–	–
Broadkill	29-Mar-19	0.89	1.39	0.35
	12-Jun-19	0.88	0.82	0.3
	13-Jun-19	1.1	0.66	0.58
	14-Jun-19	1.49	0.74	0.51
	22-Aug-19	1.51	1.38	0.4
	1-Oct-19	1.18	0.75	0.21

82.57 μM), respectively, while SUB DOC and POC concentrations ranged from 76.18 to 258.22 μM (median = 143.71 μM) and 21.09 to 345.06 μM (median = 80.74 μM) (Table S2, S3). DOC and POC were generally though not always enriched in the SML, with enrichment factors (EFs) ranging from 0.87 to 4.42 and 0.43 to 2.99, respectively (Table 2). The EFs of the various stations were not significantly different from each other (Wilcoxon rank sum's $p > 0.05$), though more marine-influenced sites (mid-bay and marine stations) had greater median EF_{DOC} and EF_{POC} (1.31 and 1.22) than the lower salinity sites (Murderkill and Broadkill stations), which had medians of 1.14 and 0.82, respectively.

SML samples also show consistently lower surface tensions than the underlying water, as indicated by mostly positive surface tension depression values (Table 2). The surface tension values for the SML and SUB samples ranged from 72.54 to 74.23 and 73.05 to 74.64 mN/m, respectively – well within acceptable ranges for saline samples (International Association for the Properties of Water and Steam, 2019).

3.2. FT-ICR MS DOM characterization

The FT-ICR MS molecular characterization of DOM identified approximately 26,000 molecular formulas across 46 samples. These formulas were grouped by elemental constituents (CHO, CHON, CHONS, and CHOS) and by operationally-defined compound class groups (saturated fatty acids, unsaturated aliphatics, peptide-like, carbohydrate-like, highly unsaturated aliphatics – low O, highly unsaturated aliphatics - high O, polyphenols - low O, polyphenolic - high O, and condensed aromatic compounds) after previous work (Osterholz et al., 2016). Their relative intensities were used to assess general differences in OM composition between samples (Figs. 2 & 3).

In general, the relative intensities of the assigned formulas followed a decreasing order of CHO, CHON, CHOS, and CHONS. The relative intensities of the CHO and CHON formulas were higher in the SUB samples (CHO_{median} = 71.2 % & $CHON_{median}$ = 18.0 %) compared to the SML (CHO_{median} = 69.9 % & $CHON_{median}$ = 17.1 %). The relative intensity of CHOS compounds was significantly higher in SML (median = 12.5 %) than in SUB (median = 9.6 %) samples (Wilcoxon rank sum's, $p < 0.0001$). CHONS formula abundances were similar for both sample types (SML_{median} = 1.24 % & SUB_{median} = 1.04 %). Plotting O/C ratios against H/C ratios of assigned formulas for each sample in a van Krevelen diagram assists in identifying differences within a complex DOM pool. Van Krevelen diagrams for a representative sample pair from the Marine station are presented in Fig. 2b. SML samples have significantly more formulas with a low O/C ratio (< 0.25) and a high H/C ratio (> 1.75) than corresponding SUB samples (Wilcoxon rank sum's $p < 0.0001$; SML Mean ± S.E = 37.3 ± 10.3, n = 23; SUB Mean ± S.E = 10.5 ± 1.85, n = 21). These formulas generally correspond to the unsaturated aliphatic, peptide-like compounds, and saturated fatty acid formula groups, but do not fit formulas associated with commonly measured amino acids or saturated fatty acids (Fig. S1) – highlighting the benefits of an untargeted approach for assessing SML OM.

Assessment of the operationally-defined compound classes reveals significantly higher relative intensities of unsaturated aliphatics (UA), saturated fatty acids (SFA) and peptide-like (PL) in the SML samples (UA_{median} = 7.32 %, SFA_{median} = 0.81 %, PL_{median} = 0.72 %) compared to the SUB (UA_{median} = 5.82 %, SFA_{median} = 0.22 %, PL_{median} = 0.53 %), while highly oxygenated highly unsaturated aliphatics (HUA) were significantly higher in the SUB (high-O HUA_{median} = 44.6 %) than in the SML (high-O HUA_{median} = 42.4 %) (Wilcoxon rank sum's $p < 0.05$) (Fig. 3). Differences in the compound class groups were also observed among the different sampling stations. Peptide-like and carbohydrate-like formula contributions were higher at the marine station compared to the other stations, whereas the polyphenolics and condensed aromatic formula contributions were higher at the mid-bay, Murderkill, and Broadkill stations compared to the marine station (Fig. 3). On average across all stations and sample types, highly unsaturated aliphatics (high-O = 43.8 ± 3.44 % and low-O = 39.7 ± 2.41 %) made up the majority of the assigned compound class groups, followed by unsaturated aliphatic compounds (6.8 ± 1.69 %). The remaining compound class groups were distributed in a decreasing order as follows: polyphenols-low O (3.2 ± 1.23 %), polyphenols-high O (2.7 ± 1.09 %), condensed aromatic compounds (2.3 ± 1.02 %), saturated fatty acids (0.8 ± 0.98 %), peptide-like (0.7 ± 0.33 %) and carbohydrate like (0.2 ± 0.218 %).

A PCA (Fig. 4) performed using the relative intensities of all formulas identified in each sample as input data reveals molecular compositional differences between the SML and SUB, and among the stations. PC1 explains 16 % of the variance in the data, and PC1 scores negatively correlate with salinity (r = 0.77, Spearman's $p < 0.0001$). The high salinity marine samples cluster separately from the inner-bay samples at negative PC1 scores, while the inner bay station samples show overlapping distributions between PC1 scores of −38 and 259 due to their shared terrestrial influences and wider salinity range (S = 11–27). Analysis of the PC loadings reveals that negative PC1 scores are associated with CHON formulas, as well as formulas with higher H/C ratios and higher O/C ratios (Fig. 4b). These formulas with higher H/C (> 1.5) and O/C (> 0.75) ratios are consistent with carbohydrate-like compounds. The positive PC1 scores, associated with formulas with a wide range of O/C and lower H/C ratios, are indicative of polyphenolic and condensed aromatic compounds (Fig. 4c).

PC2 describes 9 % of the variance between samples, and PC2 scores emphasize the differences between SML and SUB samples. SML samples have consistently and significantly (t-test, p = 0.006) higher PC2 scores than their corresponding SUB sample. Positive PC2 scores are associated with positive PC2 variable loadings from formulas with low O/C and high H/C ratios including a cluster of CHOS formulas primarily confined to H/C > 1.5 and O/C < 0.4 (Fig. 4d).

The relationship between salinity and DOM composition, as well as the distinct separation of the marine station from the inner bay stations in the initial PCA inspired site-specific analyses of DOM composition in order to deconvolute any SML/SUB trends which may have been obscured by salinity trends within the dataset. A PCA performed on only the samples collected at the marine station (Fig. S2) confirms observations from the initial PCA regarding differences between SML and SUB samples. In this data treatment, SML and SUB samples separate along PC1, which explained 26 % of the variation within the marine-restricted dataset. As observed for the entire dataset, the SML selects for

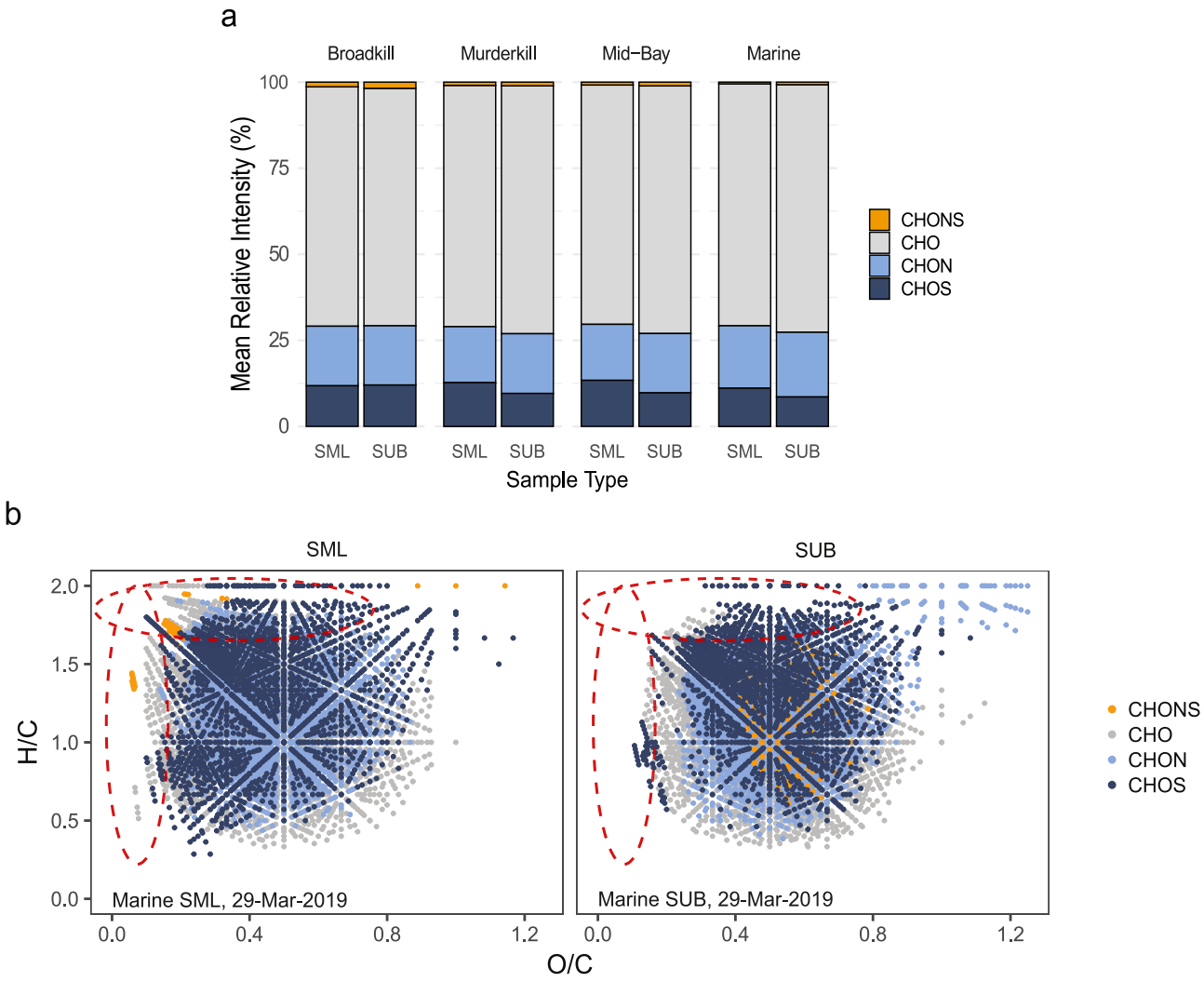

Fig. 2. a) Mean relative spectral intensities of CHO, CHON, CHONS, and CHOS formula contributions for SML and SUB samples analyzed by FT-ICR MS in this study. b) van Krevelen diagram of formulas assigned to peaks in a SML (left panel) and SUB (right panel) sample pair collected on March 29, 2019 at the marine station. Red dashed ovals call attention to regions of the van Krevelen diagram more heavily populated with formulas in SML samples (relative to SUB samples). (For interpretation of the references to colour in this figure legend, the reader is referred to the web version of this article.)

compounds with low O/C (<0.35) and high H/C (>1.5) ratios.

The trend towards lower oxygenation in the SML relative to the SUB is also observed when compound classes (CHO, CHOS, etc.) of the entire dataset are examined individually (Figs. S3–6). CHO formulas show a near-Gaussian distribution of relative intensity with oxygenation for both SML and SUB samples, with the SML's distribution being significantly (t-test, $p < 0.02$) shifted towards lower oxygenation (Fig. 5). A similar trend is observed among CHOS formulas, with a notable exception – a peak in relative intensity with CHO_3S, CHO_4S, and CHO_7S formulas. While high contributions from these formulas are present in both SML and SUB samples, they are much larger in the SML relative to SUB samples. The enhancement of signal of S-containing formulas in the SML suggests that these compounds may accumulate in the SML due to their having surfactant-like properties. Notably, linear alkylbenzene sulfonates (LAS) with C chain lengths between 10 and 14 have been identified as contaminant compounds in mass spectrometry (e.g., De Sousa et al., 2024; Matheson and Matsoim, 1983). $C_{10\text{-}14}HO_3S$ formulas of concern (Weisbrod et al., 2024) accounted for a small number ($n = 4$) of features in our samples and were eliminated from our formula lists prior to data processing and analysis. The intensity of CHO_3S features in this dataset is dominated by $C_{16\text{-}19}HO_3S$ features, carbon chain lengths consistent with a potential phytoplankton source (e.g., Morales et al., 2021), and which may be derivatives of algal sulfolipids (Fig. 6).

3.3. Fluorescent DOM composition

The relative abundance of the FDOM components varied significantly between the SML and subsurface samples (Fig. 7; Wilcoxon rank sum's $p < 0.05$). The SML exhibited consistently higher abundances of biologically derived (Peaks T and B) and photobleached (Peak H) components and lower abundances of humic-like (Peaks A, M, and C) features compared to the SUB. This is consistent with the observed higher biological index (BIX) and lower humification index (HIX) of the SML compared to the subsurface (Fig. 7g & 7h). It is also observed that the abundance of the biologically derived FDOM components increase towards the marine stations, suggesting they are of marine algal origin.

3.4. Relationships among FDOM & molecular DOM composition

Correlations between the FDOM components and various FT-ICR MS formula groups show significant (Spearman's $p < 0.05$) relationships between the two characterization techniques (Fig. S7). Polyphenolic and condensed aromatic compounds show significant negative correlations (Spearman's $p < 0.001$) with biologically-derived (BIX, Peak B, Peak T) and photobleached (Peak H) FDOM components, and significant positive correlations (Spearman's $p < 0.01$) with humic and terrestrially-derived FDOM components (HIX, Peak A, Peak C, Peak M), indicating

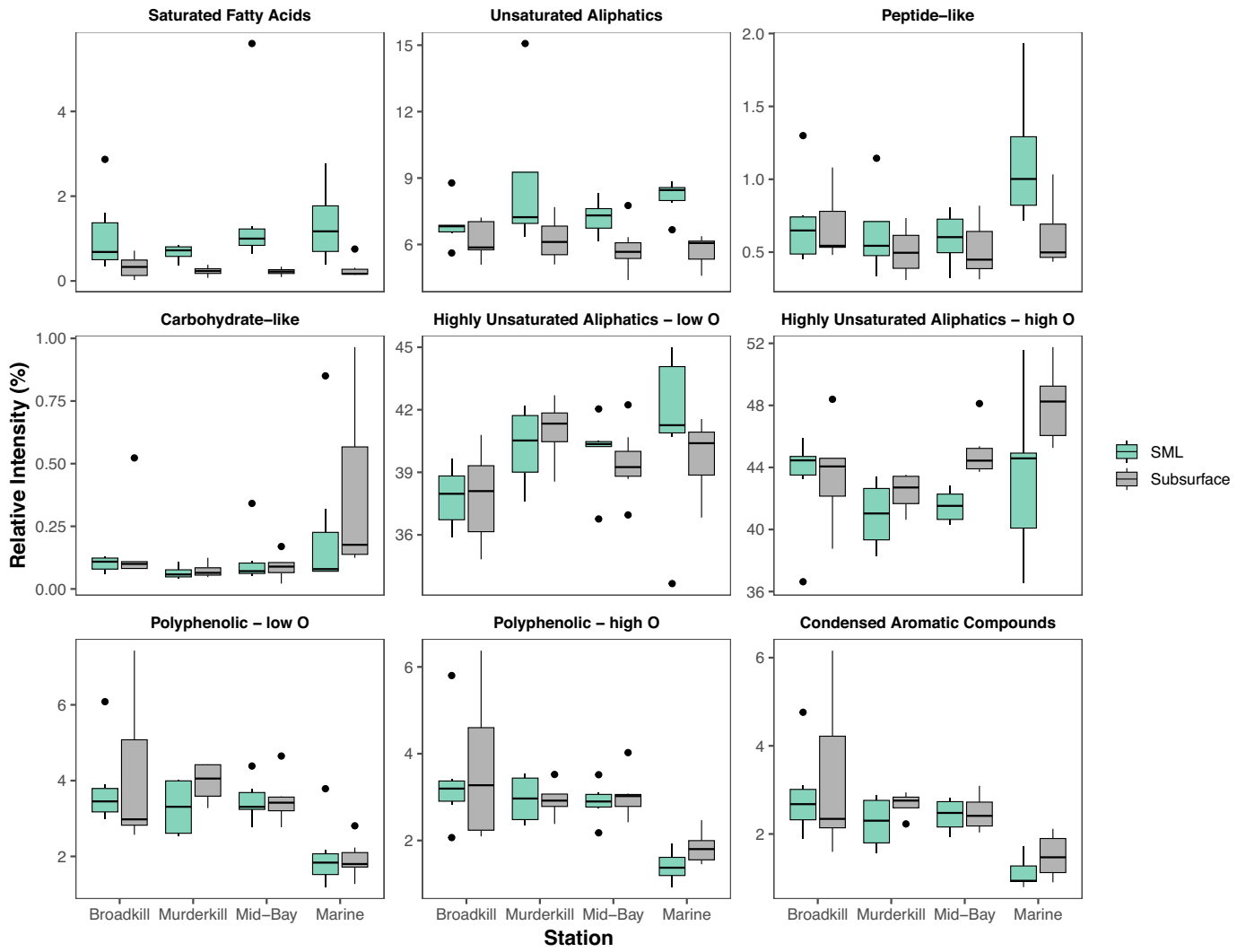

Fig. 3. Relative spectral intensities of operationally-defined compound class groups (defined at the top of each panel) identified in FT-ICR MS spectra in the SML (green) and SUB (grey) samples at each station. The lower, middle, and upper hinges of the boxplots represent the 25th, 50th (median), and 75th percentiles, respectively. The whiskers extend to the extreme data points within 1.5 times the interquartile range, while data points beyond the whiskers are considered outliers.

that these compound classes are potentially indicative of aged or otherwise degraded material. Conversely, unsaturated aliphatic compounds, peptide-like compounds, and CHO_3S formulas have significant positive correlations (Spearman's $p < 0.05$) with biologically-derived and photobleached FDOM components and significant negative correlations (Spearman's $p < 0.05$) with humic and terrestrially-derived FDOM components, potentially indicating their recent production in the SML.

3.5. Relationships between DOM composition and surface tension depression

The SML and SUB OM compositional characteristics are paired with surface tension measurements on the same samples to assess whether the OM molecular compositional differences established for the SML and SUB pair are reflected in corresponding differences in air-sea relevant properties. Salinity is known to impact surface tension; the higher the ionic strength of a solution, the higher the surface tension will be (Onsager and Samaras, 1934). In addition to this ionic effect, salt can disrupt surfactants, further raising surface tension (Qazi et al., 2020). When this entire dataset is examined, the relationship between salinity and surface tension is strong ($r = 0.62$, Spearman's $p < 0.0001$), and the wide range of salinities (11−33) likely obscures any other trends with surface tension. To control for the effects of salinity, surface tension depression, rather than raw surface tension measurements, was used in conjunction with our compositional data to investigate candidate SML surfactants. This analysis revealed 267 molecular formulas (Table S4) that were significantly (Spearman's $p < 0.05$) positively correlated with surface tension depression, many of which were unsaturated aliphatic (23.2 %) or highly unsaturated (low O, 41.2 %) compounds (Table 3). A relatively large proportion of these molecular formulas (39.7 %) contained sulfur (Table 4), indicating that sulfur-containing OM may play an important role in decreasing the surface tension of the SML. Though these individual molecular formulas showed a significant relationship with surface tension depression, the same relationship was not observed for [DOC] or [POC], highlighting the need for a compositional approach to DOM analyses when considering SML physical properties.

4. Discussion

4.1. Spatial differences in DOM composition

DOC and POC were commonly enriched in the SML, and the median EF values are in agreement with those found in estuarine and open-ocean measurements (e.g., Carlson, 1983; Huang et al., 2015; Karavoltsos et al., 2015; Lechtenfeld et al., 2013; Van Pinxteren et al.,

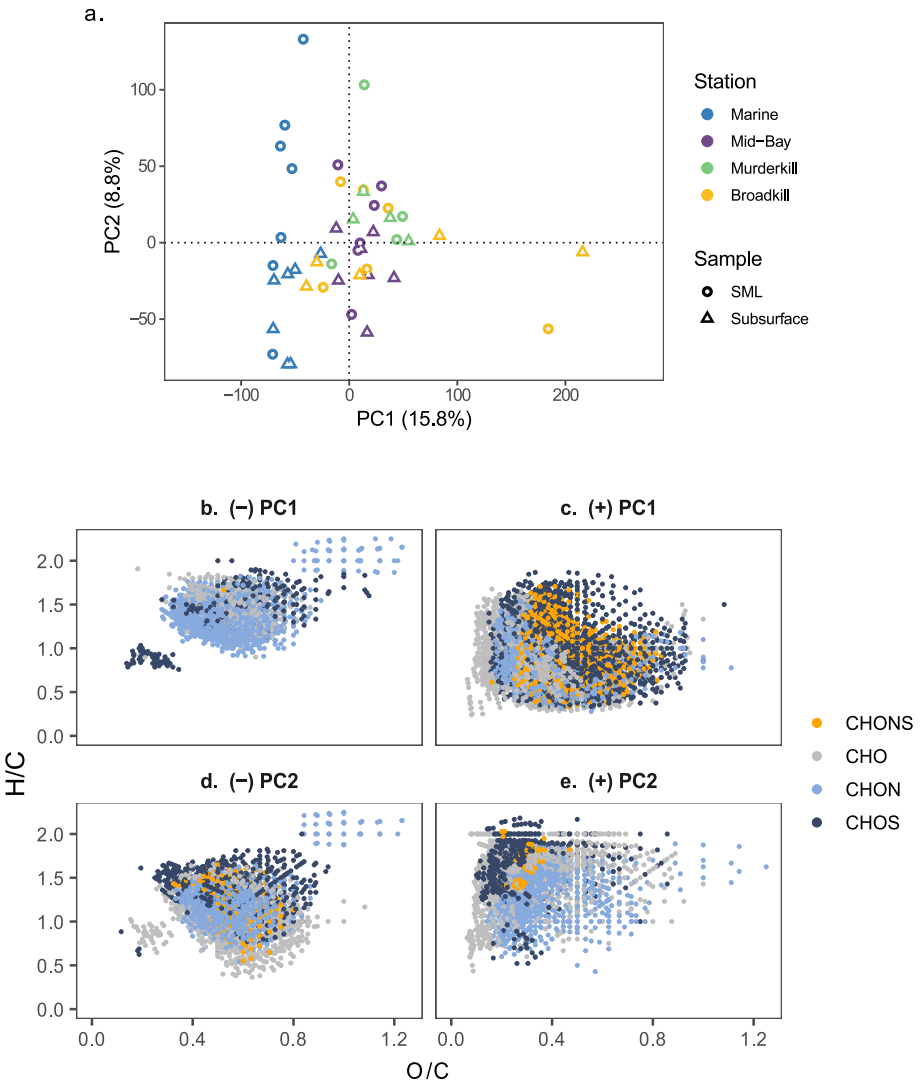

Fig. 4. a) Two-dimensional plot of PC1 (16 % of variance explained) and PC2 (9 % of variance explained) sample scores for a PCA performed using the relative intensity of formulas identified in samples from the entire dataset and van Krevelen diagrams of molecular formulas with b) negative PC1, c) positive PC1, d) negative PC2, and e) positive PC2 loadings.

2017). Though the POC EF values reported in this study are on the lower end of literature values, high OC environments such as the coastal and estuarine sites examined here tend to have lower SML enrichments (e.g., Van Pinxteren et al., 2017). Beyond bulk concentrations, fluorescent (EEMs) DOM analyses and untargeted molecular-level (FT-ICR MS) and fluorescent (EEMs) DOM analyses also revealed clear lateral (between stations) and vertical (between SML and SUB samples) spatial differences in DOM. The FDOM compositional analysis also shows preferential enrichment of biologically-derived fluorophores in the SML that correlate with the abundance of unsaturated aliphatic formulas, suggesting strong biological influence on the SML and a biological source for many of the unsaturated aliphatic formulas – consistent with previous work documenting the role of biological activity in the SML (e.g., Barthelmeß and Engel, 2022; Galgani and Engel, 2016). Additionally, the SML is enriched with photobleached FDOM (Peak H). Its position at the top of the water column exposes it to the highest amount of UV radiation where photodegradation is expected to be strongest, creating a unique environment for photochemical transformations (e.g., Rickard et al., 2022; Miranda et al., 2018; Galgani and Engel, 2016; Blough, 1997). A combination of abiotic photodegradative and biological processes are thus likely influencing the vertical gradient in DOM composition over this short depth range, and therefore also SML surfactant composition.

The SML and SUB waters display salinity-based trends in DOM and FDOM composition similar to those previously observed in the Delaware Bay (Helms et al., 2008; Osterholz et al., 2016; Powers et al., 2018) and Chesapeake Bay (Sleighter and Hatcher, 2008) that reflect a gradient in terrestrial to marine influence. At the low salinity inner bay stations, higher relative contributions from terrestrial humic-like FDOM (Fig. 7; HIX, peaks A, M) and polyphenolic and condensed aromatic formulas (Fig. 3) relative to marine stations reflect higher terrestrial-derived inputs, such as lignin-like and tannin-like material. The marine stations had higher apparent contributions from protein-like and carbohydrate-like formulas (Fig. 3) and biologically-influenced FDOM (Fig. 7; BIX, peaks B, T) that are suggestive of marine autotrophic DOM inputs (Sleighter and Hatcher, 2008). Chlorophyll-a concentrations derived from the Moderate Resolution Imaging Spectroradiometer (MODIS, NASA Aqua satellite; Wang and Shi, 2007; Werdell et al., 2007) indicate that chlorophyll-a concentrations were consistently between 10 and 30 mg/m^3 on sampling dates with available data, which would support a significant biological contribution to the DOM pool. These trends are expected for SUB waters; the similar trends observed in the SML reflect

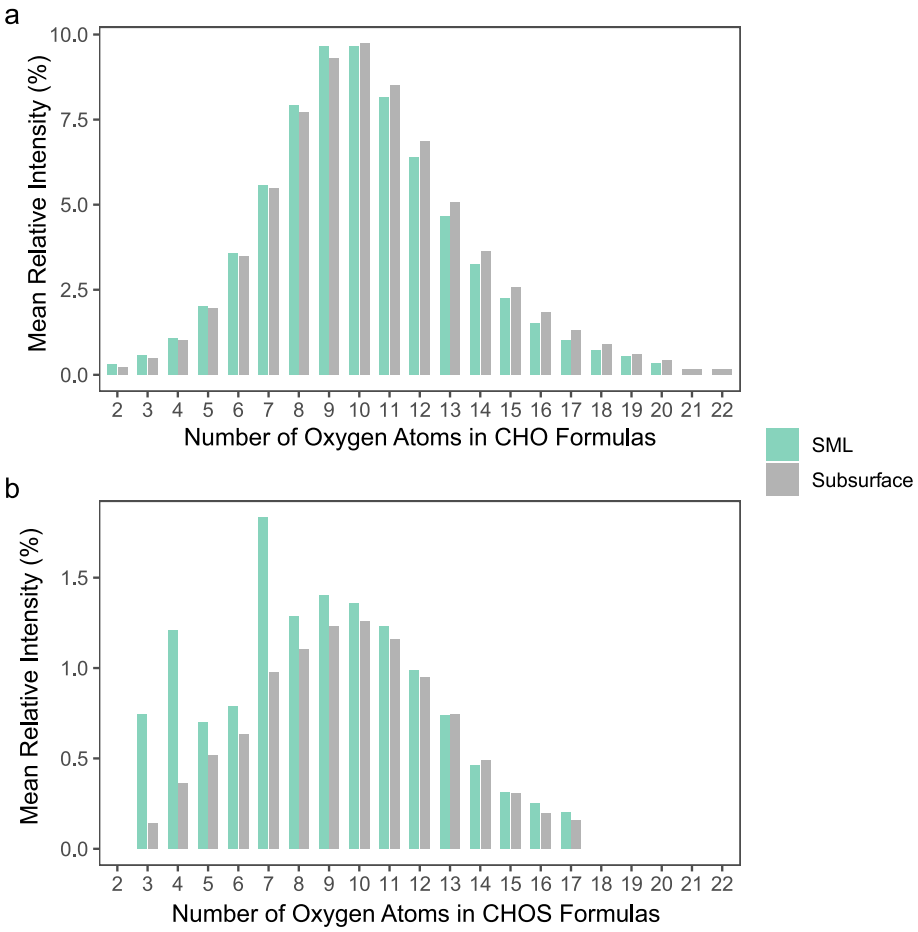

Fig. 5. Distribution of mean relative intensity contributions (% of total spectral intensity) for a) CHO formulas and b) CHOS formulas of all SML and SUB samples categorized by the number of oxygen atoms in each molecular formula.

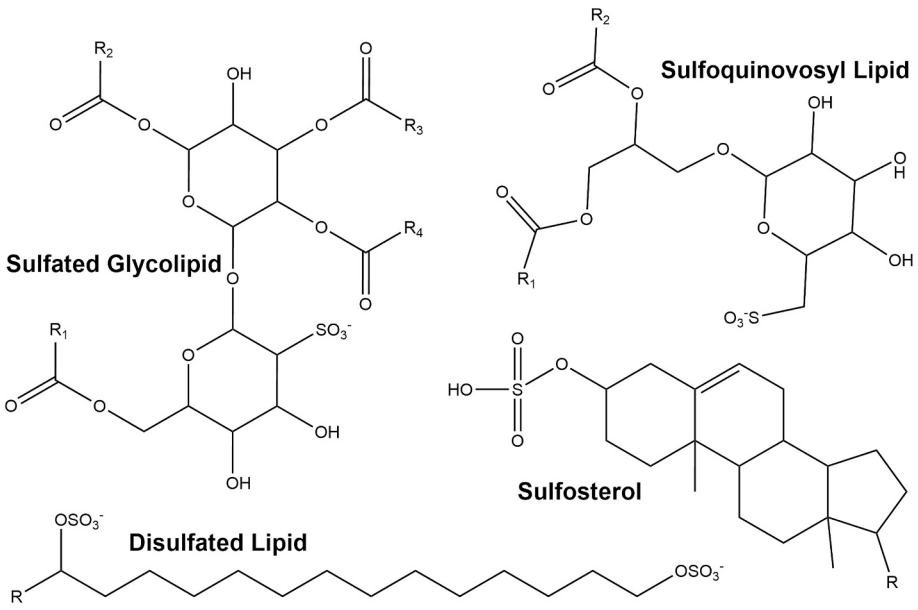

Fig. 6. Structural backbones of S–containing surfactant-like molecules, including bacterially-produced sulfated glycolipids (e.g., Mougous et al., 2004), marine algal-derived sulfoquinovosyl lipids (e.g., El Baz et al., 2013; Longnecker and Kujawinski, 2017), algal-derived sulfosterols (e.g., Gallo et al., 2017; Kates et al., 1978; Nuzzo et al., 2018), and diatom-produced disulfated lipids (e.g., Bedke and Vanderwal, 2011; Haines, 1970).

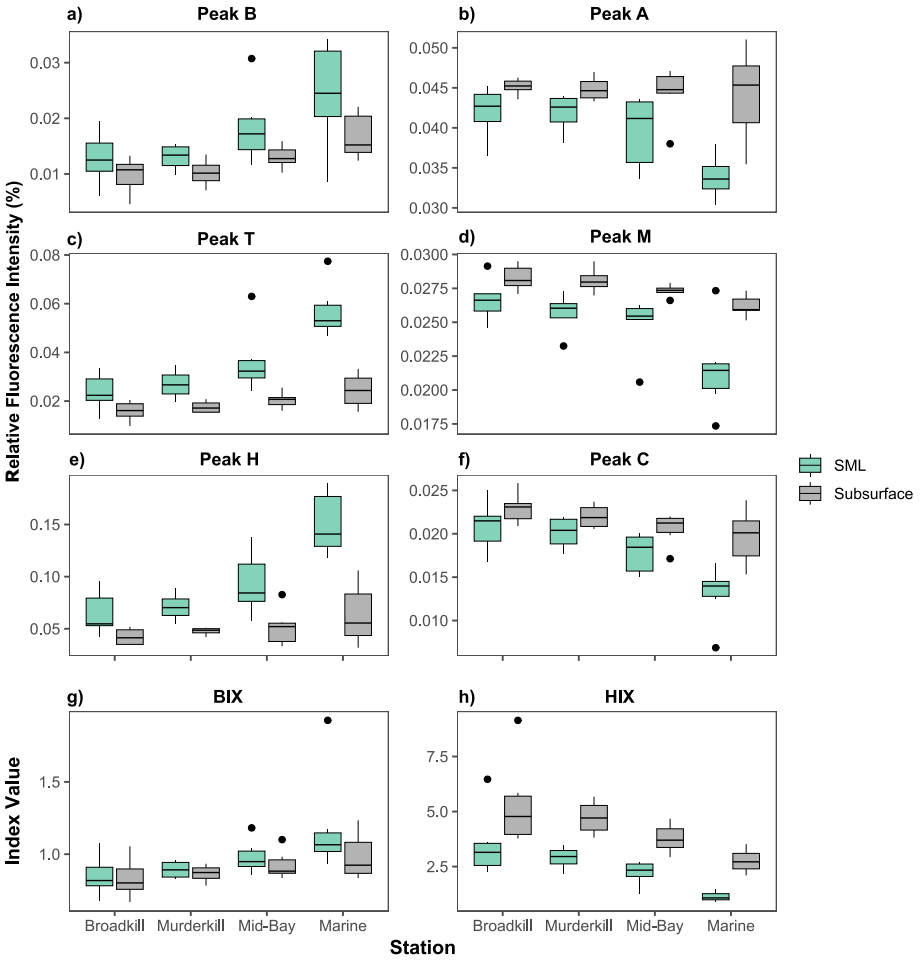

Fig. 7. Relative fluorescent intensities of major fluorophoric components a) Peak B; b) Peak A; c) Peak T; d) Peak M; e) Peak H; f) Peak C; and g) BIX and h) HIX values of SML and SUB samples as calculated from the EEMs data. The lower, middle, and upper hinges of the boxplots represent the 25th, 50th (median), and 75th percentiles, respectively. The whiskers extend to the extreme data points within 1.5 times the interquartile range, while data points beyond the whiskers are considered outliers.

Table 3
Compound classes of molecular formulas significantly (Spearman's $p < 0.05$) correlated with surface tension depression ($n = 267$).

Compound Class	# of Formulas	% of Significant Formulas
Highly Unsaturated Aliphatics – Low O	110	41.2
Unsaturated Aliphatics	62	23.2
Polyphenolic – Low O	32	12.0
Highly Unsaturated Aliphatics – High O	29	10.9
Condensed Aromatics	26	9.74
Polyphenolic – High O	6	2.25
Peptide-like	1	0.375
Saturated Fatty Acids	1	0.375

Table 4
Formula classes of molecular formulas significantly (Spearman's $p < 0.051/3$) correlated with surface tension depression ($n = 134$).

Formula Class	# of Formulas	% of Significant Formulas
CHOS	98	36.7
CHO	81	30.3
CHON	80	30.0
CHONS	8	3.00

that the influence of salinity (and the associated gradient in terrestrial-marine influence) on SUB waters also influence the SML.

In addition to the salinity-based spatial differences in DOM composition, the FT-ICR MS data reveal 166 formulas (representing an unknown number of molecular structures) with low O/C ratios (< 0.25) and high H/C ratios (> 1.75) associated with positive sample PC2 scores, and by extension, the SML. These compounds can be generally classified as saturated fatty acid, unsaturated aliphatic, or peptide-like molecules (Hockaday et al., 2009; Ohno et al., 2010; Rivas-Ubach et al., 2018; Sleighter and Hatcher, 2011; Sleighter and Hatcher, 2008) – categories linked with surfactant activity based on their likelihood of having a hydrophilic, polar functional group and a hydrophobic alkyl, alicylic, or aromatic functionality. These results are consistent with previous work documenting enrichments of biologically-derived lipids, amino acids, fatty acids, and wax esters in the SML (Brinis et al., 2004; Engel and Galgani, 2016; Frew et al., 2006; Myklestad, 1974; Nichols and Espey, 1991; Penezić et al., 2022; Sakugawa and Handa, 1985; Tilstone et al., 2010; Zäncker et al., 2017), and suggest that there is a large pool of candidate molecules to investigate regarding surfactant activity.

4.2. SML surface tension depression and candidate surfactant compounds

Bulk measurements of DOC and POC concentrations and their enrichment factors did not show significant correlations when paired with surface tension depression (Spearman's $p > 0.05$). Thus, the quantity of OM or bulk OM measurements (eg. POC and DOC) in the

SML appears to be less important than the OM composition for imparting surface-active properties (Garabetian et al., 1993; Gašparović et al., 2008) and are unreliable predictors of surface tension and surface tension depression in natural systems. Rather, the surface tension depressions in the SML are due to the enrichment in surfactant molecules in the SML as has been suggested in previous studies (e.g., Huang et al., 2015; Karavoltsos et al., 2015; Lechtenfeld et al., 2013). Indeed, laboratory and field studies have shown that the physical properties such as surface tension depression and rates of gas exchange at the air-sea interface are more heavily impacted by surfactants with lower O/C and higher H/C ratios (Burdette et al., 2022; Goldman et al., 1988; Masutani and Stenstrom, 1991) – similar to compounds seen in the SML in this study. Any efforts to model organic matter effects on surface tension properties should therefore consider DOM composition. Previous work has modelled surfactant impacts on air-sea gas exchange from presumed relationships between satellite-derived primary production and surfactant concentration (Wurl et al., 2011) and a preliminary biogeographic description of DOM (Elliott et al., 2014). More recent work has shifted to a more direct approach, with in-situ measurements of surfactant concentrations and gas transfer velocity being used to assess the SML's impact on gas exchange (Mustaffa et al., 2020).

Our work builds on these advances by deploying the 9.4 T ESI FT-ICR MS analyses to demonstrate how detailed molecular level examination of the SML surfactant pool can elucidate relationships with surface activity. Unsaturated aliphatic compounds and CHOS formulas were the major formula classifications that showed significant correlations (Spearman's $p < 0.05$) with surface tension depression for all data treatments. These molecules are expected to have amphiphilic character, and therefore fit the description of surfactant molecules expected to disrupt and decrease the surface tension of saline samples. It is quite reasonable that their presence in the SML would result in surface tension depression, and their correlation with surface tension depression across all four stations suggests that they may be useful as ubiquitous surfactant markers, within Delaware Bay and similar environments.

Though accumulation of anthropogenic surfactants in the SML has been previously reported in upper-estuarine locations (Lechtenfeld et al., 2013), the universal accumulation of CHOS compounds in the SML relative to subsurface waters is novel to this work. Potential sources for these unsaturated aliphatic, sulfur-containing surfactants include: 1) biologically-produced sulfolipid compounds and their degradation products known to be produced by algae and bacteria (El Baz et al., 2013; Longnecker and Kujawinski, 2017; Woznica et al., 2016); 2) photochemical alcohol sulfate esterification reactions at the SML as has been observed for atmospheric aerosols (Minerath et al., 2008); and 3) the allochthonous delivery of sulfur-containing surfactants via riverine transport as has been proposed in previous work (Lechtenfeld et al., 2013) or via atmospheric deposition. High H/C, low O/C CHOS formula abundances were observed to be more abundant in the SML but no apparent preference with salinity was observed (Figs. 2, 4) suggesting them to be ubiquitous over a range of salinities. Given the lack of a trend with distance from pollution sources, we reason the biological and photochemical sources to be more likely.

Biologically-derived DOM is often enriched with lipid-like materials, and the EEMs data in this study also show consistent enrichment in the relative abundance of the tyrosine peak (ex: 230, em: 305) consistent with enhanced biological production. Sulfolipid compounds have been shown to be produced by primary producers in response to phosphorus-deficient conditions including cyanobacteria (Van Mooy et al., 2006), diatoms (Dyhrman et al., 2012), and dinoflagellates (Shi et al., 2017), all of which have been observed to be abundant in Delaware Bay (Kirchman et al., 2017). Phosphorus availability was not monitored in this study. Notably, Poulson-Ellestad et al. (2014) observed sulfolipid production by diatoms under phosphorus-replete conditions but stressed by harmful algae, suggesting that sulfolipid production may not solely depend on phosphorus depletion. Other studies suggest that additional stressors such as light stress and temperature can alter the composition of algal lipids including sulfoquinovosyl diacylglycerols (Zhang et al., 2024; Li-Beisson et al., 2019). As high light intensity is a significant stressor for SML communities (e.g., Mustaffa et al., 2020; Maki, 2003; Williams et al., 1986), the role of light in controlling DOM composition in the SML should not be neglected. Further investigation into the sources, concentrations, structural identities, and roles of sulfur-containing compounds, especially sulfolipids, in microlayer composition and properties is warranted to gain a better understanding of their influence on the microlayer.

To investigate the potential role of lipids (including sulfolipids) as surfactants in our dataset, we compared the formulas that significantly correlated with surface tension depression to the LIPID MAPS® (Conroy et al., 2024) Computationally-generated Bulk Lipids database (COMP_DB) using a mass tolerance of ±0.0005. This analysis yielded a total of 179 MS^1 matches to possible lipids for 85 unique masses (32 % of the 267 formulas that correlated with surface tension depression). Sterols accounted for 117 (65 %) of these candidate lipids, including 31 sulfosterols (Table S5). Some algal species are known to produce sulfosterol-like lipids (Gallo et al., 2017; Kates et al., 1978; Nuzzo et al., 2018) indicating a likely biological source for these molecules in the SML. While, the ESI FT-ICR MS technique used in this study does not provide structural information able to verify the identities of the molecules associated with the formula assignments, sterol and sulfosterol lipids (Fig. 6) are intriguing candidates for further study as SML surfactants that influence air-sea exchanges. Structural verifications and biological origins of as well as the conditions that enhance release of these surfactants into the SML OM pool are important areas for future investigations.

4.3. Implications for our understanding of the surface microlayer

This study introduces a novel combination of high-resolution molecular characterization and surface tension measurements to the body of surface microlayer literature. Pairing the untargeted, high-resolution FT-ICR MS compositional measurements with surface tension measurements enabled the identification of hundreds of molecular formulas (and likely thousands of potential compounds) associated with surface tension depression. While structural confirmations are needed, sterols and sulfosterols emerged from this dataset as intriguing candidate surfactants ripe for future study. Work that can distinguish the sources for these compounds should be explored further, possibly by coupling assessments of microbial assemblages and photochemical experiments with high-resolution LC-MS techniques that can elucidate structural features not able to be distinguished with the current approach.

Relationships between the candidate surfactant molecular formula abundances and fluorescent spectroscopic features indicated potential biological or photochemical sources for these compounds, highlighting the potential role of these processes in altering physical properties of the SML. These linkages are valuable for understanding biogeochemical controls on SML OM composition, surface tension, and other physical properties that would not have been identified using more traditional, targeted approaches. The identification of oceanographic conditions preferable for the formation of such surfactants can lead to improved predictions of surface tension, turbulence, and mass transfer coefficients.

It must be noted that while the solid phase extraction and negative ionization mode ESI FT-ICR MS approach for analyzing the SML and SUB samples here yielded a tremendous amount of molecular information, it is not comprehensive, and many surfactants within our samples likely went uncharacterized. In particular, nonpolar compounds and compounds with basic functional groups (e.g., amino groups), including important biological compounds like amino acids, will not have been detected using this technique. Untargeted characterizations using positive mode electrospray ionization or other ionization approaches may provide further insights into surfactant identities.

The DOM compositional measurements demonstrated spatial differences in SML composition along a salinity transect that mirror those observed for subsurface waters, demonstrating a connection between

the composition of subsurface and SML waters. The data further reveal a consistent partitioning of DOM in the SML towards lower O/C and higher H/C compounds relative to SUB water in the same location, regardless of location and season. This consistent "preference" for lower O/C, higher H/C, and sulfur-containing compounds in the SML across all SML/SUB sample pairs, regardless of sampling location or seasonality reinforces the idea of a chemical molecular level control on DOM composition and properties within the SML.

CRediT authorship contribution statement

N.R. Coffey: Writing – review & editing, Writing – original draft, Visualization, Validation, Methodology, Investigation, Funding acquisition, Formal analysis. **F.E. Agblemanyo:** Writing – review & editing, Writing – original draft, Visualization, Validation, Formal analysis, Data curation. **A.M. McKenna:** Writing – review & editing, Validation, Resources, Methodology, Investigation. **A.S. Wozniak:** Writing – review & editing, Writing – original draft, Validation, Supervision, Methodology, Funding acquisition, Formal analysis, Conceptualization.

Acknowledgements and funding

A portion of this work was performed at the National High Magnetic Field Laboratory (NHMFL) ICR User Facility, which is supported by the National Science Foundation Division of Chemistry and Division of Materials Research through DMR-2128556 and the State of Florida. This work was also supported by funding from the University of Delaware Research Foundation and the U.S. National Science Foundation (OCE-2123368) to ASW and the Carolyn Thompson Thoroughgood Graduate Research Fund (supported by Dr. and Mrs. Boyer) to NRC. The authors thank Jon Swallow, Captain Kevin Beam, and the R/V Joanne Daiber for facilitating all sampling. They also thank Jessica Czarnecki, Dr. Alina Ebling, Emily Kaiser, Cissy Ming, and Dr. Amanda Frossard's research group for sampling assistance. Thanks also to Gerald Poirier and the University of Delaware's Advanced Materials Characterization Laboratory (AMCL) for allowing access to the instrumentation needed to collect surface tension data. The authors thank Dr. Jennifer Biddle and Dr. George W. Luther for their comments on early versions of the manuscript. The authors declare no competing interests.

Appendix A. Supplementary data

Supplementary data to this article can be found online at https://doi.org/10.1016/j.marchem.2025.104547.

Data availability

FT-ICR MS work was performed at the National High Magnetic Field Laboratory. All software used for FT-ICR MS data processing are publicly available: https://nationalmaglab.org/user-facilities/icr/icr-software. FT-ICR MS data presented in this paper are available via the Open Science Framework (OSF P19159 Environmental Controls on the Chemical Composition of Delaware Bay's Surface Microlayer; https://osf.io/cu9dh/). EEMs data and additional sample information are also available via the Open Science Framework.

References

Barthelmeß, T., Engel, A., 2022. How biogenic polymers control surfactant dynamics in the surface microlayer: insights from a coastal Baltic Sea study. Biogeosciences 19, 4965–4992. https://doi.org/10.5194/bg-19-4965-2022.

Bedke, D.K., Vanderwal, C.D., 2011. Chlorosulfolipids: structure, synthesis, and biological relevance. Nat. Prod. Rep. 28, 15–25. https://doi.org/10.1039/C0NP00044B.

Bercovici, S.K., Dittmar, T., Niggemann, J., 2022. The detection of bacterial exometabolites in marine dissolved organic matter through ultrahigh-resolution mass spectrometry. Limnol. Oceanogr. Methods 20, 350–360. https://doi.org/10.1002/lom3.10491.

Bittar, T.B., Stubbins, A., Vieira, A.A.H., Mopper, K., 2015a. Characterization and photodegradation of dissolved organic matter (DOM) from a tropical lake and its dominant primary producer, the cyanobacteria *Microcystis aeruginosa*. Mar. Chem. 177, 205–217. https://doi.org/10.1016/j.marchem.2015.06.016.

Bittar, T.B., Vieira, A.A.H., Stubbins, A., Mopper, K., 2015b. Competition between photochemical and biological degradation of dissolved organic matter from the cyanobacteria *Microcystis aeruginosa*. Limnol. Oceanogr. 60, 1172–1194. https://doi.org/10.1002/lno.10090.

Blakney, G.T., Hendrickson, C.L., Marshall, A.G., 2011. Predator data station: a fast data acquisition system for advanced FT-ICR MS experiments. Int. J. Mass Spectrom. 306, 246–252. https://doi.org/10.1016/j.ijms.2011.03.009.

Blough, N.V., 1997. Photochemistry in the sea-surface microlayer. In: Liss, P.S., Duce, R. A. (Eds.), The Sea Surface and Global Change. Cambridge University Press, pp. 383–424. https://doi.org/10.1017/CBO9780511525025.014.

Boldin, I.A., Nikolaev, E.N., 2011. Fourier transform ion cyclotron resonance cell with dynamic harmonization of the electric field in the whole volume by shaping of the excitation and detection electrode assembly. Rapid Commun. Mass Spectrom. 25, 122–126. https://doi.org/10.1002/rcm.4838.

Brinis, A., Méjanelle, L., Momzikoff, A., Gondry, G., Fillaux, J., Point, V., Saliot, A., 2004. Phospholipid ester-linked fatty acids composition of size-fractionated particles at the top ocean surface. Org. Geochem. 35, 1275–1287. https://doi.org/10.1016/j.orggeochem.2004.04.009.

Burdette, T.C., Bramblett, R.L., Deegan, A.M., Coffey, N.R., Wozniak, A.S., Frossard, A.A., 2022. Organic signatures of surfactants and organic molecules in surface microlayer and subsurface water of Delaware Bay. ACS Earth Space Chem. 6, 2929–2943. https://doi.org/10.1021/acsearthspacechem.2c00220.

Carlson, D.J., 1983. Dissolved organic materials in surface microlayers: temporal and spatial variability and relation to sea state. Limnol. Oceanogr. 28, 415–431. https://doi.org/10.4319/lo.1983.28.3.0415.

Carpenter, L.J., Archer, S.D., Beale, R., 2012. Ocean-atmosphere trace gas exchange. Chem. Soc. Rev. 41, 6473. https://doi.org/10.1039/c2cs35121h.

Chen, T., Beu, S.C., Kaiser, N.K., Hendrickson, C.L., 2014. Note: optimized circuit for excitation and detection with one pair of electrodes for improved Fourier transform ion cyclotron resonance mass spectrometry. Rev. Sci. Instrum. 85, 066107. https://doi.org/10.1063/1.4883179.

Chen, Y., Yang, G.-P., Xia, Q.-Y., Wu, G.-W., 2016. Enrichment and characterization of dissolved organic matter in the surface microlayer and subsurface water of the South Yellow Sea. Mar. Chem. 182, 1–13. https://doi.org/10.1016/j.marchem.2016.04.001.

Coble, P.G., 1996. Characterization of marine and terrestrial DOM in seawater using excitation-emission matrix spectroscopy. Mar. Chem. 51, 325–346. https://doi.org/10.1016/0304-4203(95)00062-3.

Conroy, M.J., Andrews, R.M., Andrews, S., Cockayne, L., Dennis, E.A., Fahy, E., Gaud, C., Griffiths, W.J., Jukes, G., Kolchin, M., Mendivelso, K., Lopez-Clavijo, A.F., Ready, C., Subramaniam, S., O'Donnell, V.B., 2024. LIPID MAPS: update to databases and tools for the lipidomics community. Nucleic Acids Res. 52, D1677–D1682. https://doi.org/10.1093/nar/gkad896.

Corilo, Y.E., 2014. PetroOrg.

Cunliffe, M., Harrison, E., Salter, M., Schäfer, H., Upstill-Goddard, R., Murrell, J., 2009. Comparison and validation of sampling strategies for the molecular microbial analysis of surface microlayers. Aquat. Microb. Ecol. 57, 69–77. https://doi.org/10.3354/ame01330.

Cunliffe, M., Upstill-Goddard, R.C., Murrell, J.C., 2011. Microbiology of aquatic surface microlayers. FEMS Microbiol. Rev. 35, 233–246. https://doi.org/10.1111/j.1574-6976.2010.00246.x.

D'Andrilli, J., Silverman, V., Buckley, S., Rosario-Ortiz, F.L., 2022. Inferring ecosystem function from dissolved organic matter optical properties: a critical review. Environ. Sci. Technol. 56, 11146–11161. https://doi.org/10.1021/acs.est.2c04240.

De Sousa, H.S., Arruda-Santos, R., Zanardi-Lamardo, E., Suarez, W.T., De Oliveira, J.L., Farias, R.A., Bezerra Dos Santos, V., 2024. A novel *in situ* method for linear alkylbenzene sulfonate quantification in environmental samples using a digital image-based method. Anal. Methods 16, 2009–2018. https://doi.org/10.1039/D4AY00073K.

Del Vento, S., Dachs, J., 2007. Influence of the surface microlayer on atmospheric deposition of aerosols and polycyclic aromatic hydrocarbons. Atmos. Environ. 41, 4920–4930. https://doi.org/10.1016/j.atmosenv.2007.01.062.

Dittmar, T., Koch, B., Hertkorn, N., Kattner, G., 2008. A simple and efficient method for the solid-phase extraction of dissolved organic matter (SPE-DOM) from seawater. Limnol. Oceanogr. Methods 6, 230–235. https://doi.org/10.4319/lom.2008.6.230.

Dreshchinskii, A., Engel, A., 2017. Seasonal variations of the sea surface microlayer at the Boknis Eck times Series Station (Baltic Sea). J. Plankton Res. 39, 943–961. https://doi.org/10.1093/plankt/fbx055.

Dyhrman, S.T., Jenkins, B.D., Rynearson, T.A., Saito, M.A., Mercier, M.L., Alexander, H., Whitney, L.P., Drzewianowski, A., Bulygin, V.V., Bertrand, E.M., Wu, Z., Benitez-Nelson, C., Heithoff, A., 2012. The transcriptome and proteome of the diatom *Thalassiosira pseudonana* reveal a diverse phosphorus stress response. PLoS One 7, e33768. https://doi.org/10.1371/journal.pone.0033768.

El Baz, F.K., El Baroty, G.S., Abd El Baky, H.H., Abd El-Salam, O.I., Ibrahim, E.A., 2013. Structural characterization and biological activity of Sulfolipids from selected marine algae. Grasas Aceites 64, 561–571. https://doi.org/10.3989/gya.050213.

Elliott, S., Burrows, S.M., Deal, C., Liu, X., Long, M., Ogunro, O., Russell, L.M., Wingenter, O., 2014. Prospects for simulating macromolecular surfactant chemistry at the ocean–atmosphere boundary. Environ. Res. Lett. 9, 064012. https://doi.org/10.1088/1748-9326/9/6/064012.

Emmett, M.R., White, F.M., Hendrickson, C.L., Shi, S.D.-H., Marshall, A.G., 1998. Application of micro-electrospray liquid chromatography techniques to FT-ICR MS

to enable high-sensitivity biological analysis. J. Am. Soc. Mass Spectrom. 9, 333–340. https://doi.org/10.1016/S1044-0305(97)00287-0.
Engel, A., Galgani, L., 2016. The organic sea-surface microlayer in the upwelling region off the coast of Peru and potential implications for air–sea exchange processes. Biogeosciences 13, 989–1007. https://doi.org/10.5194/bg-13-989-2016.
Frew, N.M., 1997. The role of organic films in air–sea gas exchange. In: Liss, P.S., Duce, R.A. (Eds.), The Sea Surface and Global Change. Cambridge University Press, pp. 121–172. https://doi.org/10.1017/CBO9780511525025.006.
Frew, N.M., Goldman, J.C., Dennett, M.R., Johnson, A.S., 1990. Impact of phytoplankton-generated surfactants on air-sea gas exchange. J. Geophys. Res. 95, 3337–3352. https://doi.org/10.1029/JC095iC03p03337.
Frew, N.M., Bock, E.J., Schimpf, U., Hara, T., Haußecker, H., Edson, J.B., McGillis, W.R., Nelson, R.K., McKenna, S.P., Uz, B.M., Jähne, B., 2004. Air-sea gas transfer: its dependence on wind stress, small-scale roughness, and surface films. J. Geophys. Res. 109, 2003JC002131. https://doi.org/10.1029/2003JC002131.
Frew, N.M., Nelson, R.K., Johnson, C.G., 2006. Sea slicks: Variability in chemical composition and surface elasticity. In: Gade, M., Hühnerfuss, H., Korenowski, G.M. (Eds.), Marine Surface Films. Springer-Verlag, Berlin/Heidelberg, pp. 45–56. https://doi.org/10.1007/3-540-33271-5_6.
Frossard, A.A., Gérard, V., Duplessis, P., Kinsey, J.D., Lu, X., Zhu, Y., Bisgrove, J., Maben, J.R., Long, M.S., Chang, R.Y.-W., Beaupré, S.R., Kieber, D.J., Keene, W.C., Nozière, B., Cohen, R.C., 2019. Properties of seawater surfactants associated with primary marine aerosol particles produced by bursting bubbles at a model air–sea interface. Environ. Sci. Technol. 53, 9407–9417. https://doi.org/10.1021/acs.est.9b02637.
Galgani, L., Engel, A., 2016. Changes in optical characteristics of surface microlayers hint to photochemically and microbially mediated DOM turnover in the upwelling region off the coast of Peru. Biogeosciences 13, 2453–2473. https://doi.org/10.5194/bg-13-2453-2016.
Gallo, C., d'Ippolito, G., Nuzzo, G., Sardo, A., Fontana, A., 2017. Autoinhibitory sterol sulfates mediate programmed cell death in a bloom-forming marine diatom. Nat. Commun. 8, 1292. https://doi.org/10.1038/s41467-017-01300-1.
Gantt, B., Meskhidze, N., 2013. The physical and chemical characteristics of marine primary organic aerosol: a review. Atmos. Chem. Phys. 13, 3979–3996. https://doi.org/10.5194/acp-13-3979-2013.
Garabetian, F., Romano, J.-C., Paul, R., Sigoillot, J.-C., 1993. Organic matter composition and pollutant enrichment of sea surface microlayer inside and outside slicks. Mar. Environ. Res. 35, 323–339. https://doi.org/10.1016/0141-1136(93)90100-E.
Gašparović, B., Frka, S., Kozarac, Z., Nelson, A., 2008. A method for characterization of sea surface microlayer based on monolayer properties in presence and absence of phospholipids. Anal. Chim. Acta 620, 64–72. https://doi.org/10.1016/j.aca.2008.05.043.
Goldman, J.C., Dennett, M.R., Frew, N.M., 1988. Surfactant effects on air-sea gas exchange under turbulent conditions. Deep-Sea Res. Part A Oceanogr. Res. Pap. 35, 1953–1970. https://doi.org/10.1016/0198-0149(88)90119-7.
Haines, T.H., 1970. Algal Sulfolipids and Chlorosulfolipids. In: Zajic, J.E. (Ed.), Properties and Products of Algae. Springer US, Boston, MA, pp. 129–142. https://doi.org/10.1007/978-1-4684-1824-8_7.
Harvey, G.W., 1966. Microlayer collection from the sea surface: a new method and initial results1. Limnol. Oceanogr. 11, 608–613. https://doi.org/10.4319/lo.1966.11.4.0608.
Harvey, G.W., Burzell, L.A., 1972. A simple microlayer method for small samples1. Limnol. Oceanogr. 17, 156–157. https://doi.org/10.4319/lo.1972.17.1.0156.
Helms, J.R., Stubbins, A., Ritchie, J.D., Minor, E.C., Kieber, D.J., Mopper, K., 2008. Absorption spectral slopes and slope ratios as indicators of molecular weight, source, and photobleaching of chromophoric dissolved organic matter. Limnol. Oceanogr. 53, 955–969. https://doi.org/10.4319/lo.2008.53.3.0955.
Hockaday, W.C., Purcell, J.M., Marshall, A.G., Baldock, J.A., Hatcher, P.G., 2009. Electrospray and photoionization mass spectrometry for the characterization of organic matter in natural waters: a qualitative assessment. Limnol. Oceanogr. Methods 7, 81–95. https://doi.org/10.4319/lom.2009.7.81.
Huang, Y.-J., Brimblecombe, P., Lee, C.-L., Latif, M.T., 2015. Surfactants in the sea-surface microlayer and sub-surface water at estuarine locations: their concentration, distribution, enrichment, and relation to physicochemical characteristics. Mar. Pollut. Bull. 97, 78–84. https://doi.org/10.1016/j.marpolbul.2015.06.031.
Hughey, C.A., Hendrickson, C.L., Rodgers, R.P., Marshall, A.G., Qian, K., 2001. Kendrick mass defect Spectrum: a compact visual analysis for ultrahigh-resolution broadband mass spectra. Anal. Chem. 73, 4676–4681. https://doi.org/10.1021/ac010560w.
Huguet, A., Vacher, L., Relexans, S., Saubusse, S., Froidefond, J.M., Parlanti, E., 2009. Properties of fluorescent dissolved organic matter in the Gironde estuary. Org. Geochem. 40, 706–719. https://doi.org/10.1016/j.orggeochem.2009.03.002.
International Association for the Properties of Water and Steam, 2019. Guideline on the surface tension of seawater. IAPWS G14–19.
Jaafar, S.A., Latif, M.T., Chian, C.W., Han, W.S., Wahid, N.B.A., Razak, I.S., Khan, M.F., Tahir, N.M., 2014. Surfactants in the sea-surface microlayer and atmospheric aerosol around the southern region of peninsular Malaysia. Mar. Pollut. Bull. 84, 35–43. https://doi.org/10.1016/j.marpolbul.2014.05.047.
Jenkinson, I.R., Seuront, L., Ding, H., Elias, F., 2018. Biological modification of mechanical properties of the sea surface microlayer, influencing waves, ripples, foam and air-sea fluxes. Elementa Sci. Anthrop. 6, 26. https://doi.org/10.1525/elementa.283.
Jun, L., Hai-bing, D., Zhi-jian, W., Zheng-bin, Z., Lian-sheng, L., 1998. Determination of apparent sampling thickness of sea surface microlayer. Chin. J. Oceanol. Limnol. 16, 177–182. https://doi.org/10.1007/BF02845185.
Kaiser, N.K., Quinn, J.P., Blakney, G.T., Hendrickson, C.L., Marshall, A.G., 2011. A novel 9.4 tesla FTICR mass spectrometer with improved sensitivity, mass resolution, and mass range. J. Am. Soc. Mass Spectrom. 22, 1343–1351. https://doi.org/10.1007/s13361-011-0141-9.
Kaiser, N.K., McKenna, A.M., Savory, J.J., Hendrickson, C.L., Marshall, A.G., 2013. Tailored ion radius distribution for increased dynamic range in FT-ICR mass analysis of complex mixtures. Anal. Chem. 85, 265–272. https://doi.org/10.1021/ac302678v.
Kaiser, N.K., Savory, J.J., Hendrickson, C.L., 2014. Controlled ion ejection from an external trap for extended ***m/z*** range in FT-ICR mass spectrometry. J. Am. Soc. Mass Spectrom. 25, 943–949. https://doi.org/10.1007/s13361-014-0871-6.
Karavoltsos, S., Kalambokis, E., Sakellari, A., Plavšić, M., Dotsika, E., Karalis, P., Leondiadis, L., Dassenakis, M., Scoullos, M., 2015. Organic matter characterization and copper complexing capacity in the sea surface microlayer of coastal areas of the eastern Mediterranean. Mar. Chem. 173, 234–243. https://doi.org/10.1016/j.marchem.2014.12.004.
Kates, M., Tremblay, P., Anderson, R., Volcani, B.E., 1978. Identification of the free and conjugated sterol in a non-photosynthetic diatom, *Nitzschia alba*, as 24-methylene cholesterol. Lipids 13, 34–41. https://doi.org/10.1007/BF02533364.
Kendrick, Edward, 1963. A mass scale based on $CH_2 = 14.0000$ for high resolution mass spectrometry of organic compounds. Anal. Chem. 35, 2146–2154. https://doi.org/10.1021/ac60206a048.
Kim, S., Kramer, R.W., Hatcher, P.G., 2003. Graphical method for analysis of ultrahigh-resolution broadband mass spectra of natural organic matter, the Van Krevelen diagram. Anal. Chem. 75, 5336–5344. https://doi.org/10.1021/ac034415p.
Kirchman, D., Cottrel, M., DiTullio, G., 2017. Shaping of bacterial community composition and diversity by phytoplankton and salinity in the Delaware estuary, USA. Aquat. Microb. Ecol. 78, 93–106. https://doi.org/10.3354/ame01805.
Kujawinski, E.B., 2011. The impact of microbial metabolism on marine dissolved organic matter. Annu. Rev. Mar. Sci. 3, 567–599. https://doi.org/10.1146/annurev-marine-120308-081003.
Lawaetz, A.J., Stedmon, C.A., 2009. Fluorescence intensity calibration using the Raman scatter peak of water. Appl. Spectrosc. 63, 936–940. https://doi.org/10.1366/000370209788964548.
Lechtenfeld, O.J., Koch, B.P., Gašparović, B., Frka, S., Witt, M., Kattner, G., 2013. The influence of salinity on the molecular and optical properties of surface microlayers in a karstic estuary. Mar. Chem. 150, 25–38. https://doi.org/10.1016/j.marchem.2013.01.006.
Leresche, F., Vialykh, E.A., Rosario-Ortiz, F.L., 2022. Computational calculation of dissolved organic matter absorption spectra. Environ. Sci. Technol. 56, 491–500. https://doi.org/10.1021/acs.est.1c06252.
Lewis, E.R., Schwartz, S.E. (Eds.), 2004. Sea Salt Aerosol Production: Mechanisms, Methods, Measurements and Models: A Critical Review, Geophysical Monograph. American Geophysical Union, Washington, DC.
Li-Beisson, Y., Thelen, J.J., Fedosejevs, E., Harwood, J.L., 2019. The lipid biochemistry of eukaryotic algae. Prog. Lipid Res. 74, 31–68. https://doi.org/10.1016/j.plipres.2019.01.003.
Liss, P.S., Duce, R.A. (Eds.), 1997. The Sea Surface and Global Change, 1st ed. Cambridge University Press. https://doi.org/10.1017/CBO9780511525025.
Longnecker, K., Kujawinski, E.B., 2017. Mining mass spectrometry data: using new computational tools to find novel organic compounds in complex environmental mixtures. Org. Geochem. 110, 92–99. https://doi.org/10.1016/j.orggeochem.2017.05.008.
Longnecker, K., Kido Soule, M.C., Kujawinski, E.B., 2015. Dissolved organic matter produced by *Thalassiosira pseudonana*. Mar. Chem. 168, 114–123. https://doi.org/10.1016/j.marchem.2014.11.003.
Maki, J.S., 2003. Neuston microbiology: life at the air-water interface. In: Bitton, G. (Ed.), Encyclopedia of Environmental Microbiology. https://doi.org/10.1002/0471263397.env234.
Marty, J.C., Žutić, V., Precali, R., Saliot, A., Ćosović, B., Smodlaka, N., Cauwet, G., 1988. Organic matter characterization in the northern adriatic sea with special reference to the sea surface microlayer. Mar. Chem. 25, 243–263. https://doi.org/10.1016/0304-4203(88)90053-9.
Massicotte, P., 2019. eemR: Tools for Pre-Processing Emission-Excitation-Matrix (EEM) Fluorescence Data.
Masutani, G.K., Stenstrom, M.K., 1991. Dynamic surface tension effects on oxygen transfer. J. Environ. Eng. 117, 126–142. https://doi.org/10.1061/(ASCE)0733-9372(1991)117:1(126).
Matheson, K.L., Matsoim, T.P., 1983. Effect of carbon chain and phenyl isomer distribution on use properties of linear alkylbenzene sulfonate: a comparison of 'high' and 'low' 2-phenyl LAS homologs. J. Americ. Oil Chem. Soc. 60, 1693–1698. https://doi.org/10.1007/BF02662436.
McKnight, D.M., Boyer, E.W., Westerhoff, P.K., Doran, P.T., Kulbe, T., Andersen, D.T., 2001. Spectrofluorometric characterization of dissolved organic matter for indication of precursor organic material and aromaticity. Limnol. Oceanogr. 46, 38–48. https://doi.org/10.4319/lo.2001.46.1.0038.
McLafferty, F.W., Turecek, F., 1993. Interpretation of Mass Spectra, 4th ed. University Science Books, Mill Valley, CA. https://doi.org/10.1021/ed071pA54.5.
Minerath, E.C., Casale, M.T., Elrod, M.J., 2008. Kinetics feasibility study of alcohol sulfate esterification reactions in tropospheric aerosols. Environ. Sci. Technol. 42, 4410–4415. https://doi.org/10.1021/es8004333.
Miranda, M.L., Mustaffa, N.I.H., Robinson, T.B., Stolle, C., Ribas-Ribas, M., Wurl, O., Zielinski, O., 2018. Influence of solar radiation on biogeochemical parameters and fluorescent dissolved organic matter (FDOM) in the sea surface microlayer of the southern coastal North Sea. Elem. Sci. Anth. 6, 15. https://doi.org/10.1525/elementa.278.
Mitra, S., Wozniak, A.S., Miller, R., Hatcher, P.G., Buonassissi, C., Brown, M., 2013. Multiproxy probing of rainwater dissolved organic matter (DOM) composition in

coastal storms as a function of trajectory. Mar. Chem. 154, 67–76. https://doi.org/10.1016/j.marchem.2013.05.013.
Morales, M., Aflalo, C., Bernard, O., 2021. Microalgal lipids: a review of lipids potential and quantification for 95 phytoplankton species. Biomass Bioenergy 150, 106108. https://doi.org/10.1016/j.biombioe.2021.106108.
Moran, M.A., Kujawinski, E.B., Stubbins, A., Fatland, R., Aluwihare, L.I., Buchan, A., Crump, B.C., Dorrestein, P.C., Dyhrman, S.T., Hess, N.J., Howe, B., Longnecker, K., Medeiros, P.M., Niggemann, J., Obernosterer, I., Repeta, D.J., Waldbauer, J.R., 2016. Deciphering Ocean carbon in a changing world. Proc. Natl. Acad. Sci. USA 113, 3143–3151. https://doi.org/10.1073/pnas.1514645113.
Mougous, J.D., Petzold, C.J., Senaratne, R.H., Lee, D.H., Akey, D.L., Lin, F.L., Munchel, S. E., Pratt, M.R., Riley, L.W., Leary, J.A., Berger, J.M., Bertozzi, C.R., 2004. Identification, function and structure of the mycobacterial sulfotransferase that initiates sulfolipid-1 biosynthesis. Nat. Struct. Mol. Biol. 11, 721–729. https://doi.org/10.1038/nsmb802.
Murphy, K.R., Stedmon, C.A., Waite, T.D., Ruiz, G.M., 2008. Distinguishing between terrestrial and autochthonous organic matter sources in marine environments using fluorescence spectroscopy. Mar. Chem. 108, 40–58. https://doi.org/10.1016/j.marchem.2007.10.003.
Mustaffa, N.I.H., Ribas-Ribas, M., Wurl, O., 2017. High-resolution variability of the enrichment of fluorescence dissolved organic matter in the sea surface microlayer of an upwelling region. Elementa Sci. Anthrop. 5, 52. https://doi.org/10.1525/elementa.242.
Mustaffa, N.I.H., Badewien, T.H., Ribas-Ribas, M., Wurl, O., 2018. High-resolution observations on enrichment processes in the sea-surface microlayer. Sci. Rep. 8, 13122. https://doi.org/10.1038/s41598-018-31465-8.
Mustaffa, N.I.H., Ribas-Ribas, M., Banko-Kubis, H.M., Wurl, O., 2020. Global reduction of *in situ* CO_2 transfer velocity by natural surfactants in the sea-surface microlayer. Proc. R. Soc. A. 476, 20190763. https://doi.org/10.1098/rspa.2019.0763.
Myklestad, S., 1974. Production of carbohydrates by marine planktonic diatoms. I. Comparison of nine different species in culture. J. Exp. Mar. Biol. Ecol. 15, 261–274. https://doi.org/10.1016/0022-0981(74)90049-5.
Nichols, P.D., Espey, Q.I., 1991. Characterization of organic matter at the air-sea interface, in subsurface water, and in bottom sediments near the Malabar sewage outfall in Sydney's coastal region. Aust. J. Mar. Freshwat. Res. 42, 327–348. https://doi.org/10.1071/MF9910327.
Nuzzo, G., Gallo, C., D'Ippolito, G., Manzo, E., Ruocco, N., Russo, E., Carotenuto, Y., Costantini, M., Zupo, V., Sardo, A., Fontana, A., 2018. UPLC–MS/MS identification of sterol sulfates in marine diatoms. Mar. Drugs 17, 10. https://doi.org/10.3390/md17010010.
Ohno, T., 2002. Fluorescence inner-filtering correction for determining the Humification index of dissolved organic matter. Environ. Sci. Technol. 36, 742–746. https://doi.org/10.1021/es0155276.
Ohno, T., He, Z., Sleighter, R.L., Honeycutt, C.W., Hatcher, P.G., 2010. Ultrahigh resolution mass spectrometry and Indicator species analysis to identify marker components of soil- and plant biomass-derived organic matter fractions. Environ. Sci. Technol. 44, 8594–8600. https://doi.org/10.1021/es101089t.
Onsager, L., Samaras, N.N.T., 1934. The surface tension of Debye-Hückel electrolytes. J. Chem. Phys. 2, 528–536. https://doi.org/10.1063/1.1749522.
Osterholz, H., Kirchman, D.L., Niggemann, J., Dittmar, T., 2016. Environmental drivers of dissolved organic matter molecular composition in the Delaware estuary. Front. Earth Sci. 4. https://doi.org/10.3389/feart.2016.00095.
Penezić, A., Drozdowska, V., Novak, T., Gašparović, B., 2022. Distribution and characterization of organic matter within the sea surface microlayer in the Gulf of Gdańsk. Oceanologia 64, 631–650. https://doi.org/10.1016/j.oceano.2022.05.003.
Pereira, R., Ashton, I., Sabbaghzadeh, B., Shutler, J.D., Upstill-Goddard, R.C., 2018. Reduced air–sea CO2 exchange in the Atlantic Ocean due to biological surfactants. Nat. Geosci. 11, 492–496. https://doi.org/10.1038/s41561-018-0136-2.
Poulson-Ellestad, K.L., Jones, C.M., Roy, J., Viant, M.R., Fernández, F.M., Kubanek, J., Nunn, B.L., 2014. Metabolomics and proteomics reveal impacts of chemically mediated competition on marine plankton. Proc. Natl. Acad. Sci. USA 111, 9009–9014. https://doi.org/10.1073/pnas.1402130111.
Powers, L.C., Luek, J.L., Schmitt-Kopplin, P., Campbell, B.J., Magen, C., Cooper, L.W., Gonsior, M., 2018. Seasonal changes in dissolved organic matter composition in Delaware Bay, USA in march and august 2014. Org. Geochem. 122, 87–97. https://doi.org/10.1016/j.orggeochem.2018.05.005.
Qazi, M.J., Schlegel, S.J., Backus, E.H.G., Bonn, M., Bonn, D., Shahidzadeh, N., 2020. Dynamic surface tension of surfactants in the presence of high salt concentrations. Langmuir 36, 7956–7964. https://doi.org/10.1021/acs.langmuir.0c01211.
R Core Team, 2022. R: A Language and Environment for Statistical Computing.
Razali, N.M., Wah, Y.B., 2011. Power comparisons of shapiro-wilk, kolmogorov-smirnov, lilliefors and Anderson-darling tests. J. Stat. Model. Anal. 2 (1), 21–33.
Rickard, P.C., Uher, G., Upstill-Goddard, R.C., 2022. Photo-reactivity of surfactants in the sea-surface microlayer and subsurface water of the Tyne estuary, UK. Geophys. Res. Lett. 49, e2021GL095469. https://doi.org/10.1029/2021GL095469.
Rivas-Ubach, A., Liu, Y., Bianchi, T.S., Tolić, N., Jansson, C., Paša-Tolić, L., 2018. Moving beyond the van Krevelen diagram: a new stoichiometric approach for compound classification in organisms. Anal. Chem. 90, 6152–6160. https://doi.org/10.1021/acs.analchem.8b00529.
Sabbaghzadeh, B., Upstill-Goddard, R.C., Beale, R., Pereira, R., Nightingale, P.D., 2017. The Atlantic Ocean surface microlayer from 50°N to 50°S is ubiquitously enriched in surfactants at wind speeds up to 13 m s^{-1}. Geophys. Res. Lett. 44, 2852–2858. https://doi.org/10.1002/2017GL072988.
Sakugawa, H., Handa, N., 1985. Isolation and chemical characterization of dissolved and particulate polysaccharides in Mikawa Bay. Geochim. Cosmochim. Acta 49, 1185–1193. https://doi.org/10.1016/0016-7037(85)90009-2.
Savory, J.J., Kaiser, N.K., McKenna, A.M., Xian, F., Blakney, G.T., Rodgers, R.P., Hendrickson, C.L., Marshall, A.G., 2011. Parts-per-billion Fourier transform ion cyclotron resonance mass measurement accuracy with a "walking" calibration equation. Anal. Chem. 83, 1732–1736. https://doi.org/10.1021/ac102943z.
Shi, X., Lin, X., Li, L., Li, M., Palenik, B., Lin, S., 2017. Transcriptomic and microRNAomic profiling reveals multi-faceted mechanisms to cope with phosphate stress in a dinoflagellate. ISME J. 11, 2209–2218. https://doi.org/10.1038/ismej.2017.81.
Siddiqui, F.A., Franses, E.I., 1996. Equilibrium adsorption and tension of binary surfactant mixtures at the air/water interface. Langmuir 12, 354–362. https://doi.org/10.1021/la9506032.
Sleighter, R.L., Hatcher, P.G., 2008. Molecular characterization of dissolved organic matter (DOM) along a river to ocean transect of the lower Chesapeake Bay by ultrahigh resolution electrospray ionization Fourier transform ion cyclotron resonance mass spectrometry. Mar. Chem. 110, 140–152. https://doi.org/10.1016/j.marchem.2008.04.008.
Sleighter, R.L., Hatcher, P.G., 2011. Fourier transform mass spectrometry for the molecular level characterization of natural organic matter: instrument capabilities, applications, and limitations. In: Nikolic, G. (Ed.), Fourier Transforms - Approach to Scientific Principles. InTech. https://doi.org/10.5772/15959.
Tilstone, G.H., Airs, R.L., Vicente, V.M., Widdicombe, C., Llewellyn, C., 2010. High concentrations of mycosporine-like amino acids and colored dissolved organic matter in the sea surface microlayer off the Iberian Peninsula. Limnol. Oceanogr. 55, 1835–1850. https://doi.org/10.4319/lo.2010.55.5.1835.
Van Mooy, B.A.S., Rocap, G., Fredricks, H.F., Evans, C.T., Devol, A.H., 2006. Sulfolipids dramatically decrease phosphorus demand by picocyanobacteria in oligotrophic marine environments. Proc. Natl. Acad. Sci. USA 103, 8607–8612. https://doi.org/10.1073/pnas.0600540103.
Van Pinxteren, M., Barthel, S., Fomba, K.W., Müller, K., Von Tümpling, W., Herrmann, H., 2017. The influence of environmental drivers on the enrichment of organic carbon in the sea surface microlayer and in submicron aerosol particles – measurements from the Atlantic Ocean. Elementa Sci. Anthrop. 5, 35. https://doi.org/10.1525/elementa.225.
Wang, M., Shi, W., 2007. The NIR-SWIR combined atmospheric correction approach for MODIS Ocean color data processing. Opt. Express 15, 15722. https://doi.org/10.1364/oe.15.015722.
Weisbrod, C.R., McKenna, A.M., Hendrickson, C.L., 2024. Selective gas-phase depletion of chemical contaminants in dissolved organic matter increases compositional coverage by FT-ICR mass spectrometry. J. Am. Soc. Mass Spectrom. 35, 2465–2471. https://doi.org/10.1021/jasms.4c00261.
Werdell, P.J., Franz, B.A., Bailey, S.W., Harding Jr., L.W., Feldman, G.C., 2007. Approach for the long-term spatial and temporal evaluation of ocean color satellite data products in a coastal environment. In: Frouin, R.J. (Ed.), SPIE Proceedings. Presented at the Optical Engineering + Applications. SPIE, San Diego, CA. https://doi.org/10.1117/12.732489, 66800G.
Williams, P.M., Carlucci, A.F., Henrichs, S.M., Van Vleet, E.S., Horrigan, S.G., Reid, F.M. H., Robertson, K.J., 1986. Chemical and microbiological studies of sea-surface films in the southern gulf of California and off the west coast of Baja California. Mar. Chem. 19, 17–98.
Wilson, T.W., Ladino, L.A., Alpert, P.A., Breckels, M.N., Brooks, I.M., Browse, J., Burrows, S.M., Carslaw, K.S., Huffman, J.A., Judd, C., Kilthau, W.P., Mason, R.H., McFiggans, G., Miller, L.A., Nájera, J.J., Polishchuk, E., Rae, S., Schiller, C.L., Si, M., Temprado, J.V., Whale, T.F., Wong, J.P.S., Wurl, O., Yakobi-Hancock, J.D., Abbatt, J.P.D., Aller, J.Y., Bertram, A.K., Knopf, D.A., Murray, B.J., 2015. A marine biogenic source of atmospheric ice-nucleating particles. Nature 525, 234–238. https://doi.org/10.1038/nature14986.
Wozniak, A.S., Bauer, J.E., Dickhut, R.M., 2012. Characteristics of water-soluble organic carbon associated with aerosol particles in the eastern United States. Atmos. Environ. 46, 181–188. https://doi.org/10.1016/j.atmosenv.2011.10.001.
Woznica, A., Cantley, A.M., Beemelmanns, C., Freinkman, E., Clardy, J., King, N., 2016. Bacterial lipids activate, synergize, and inhibit a developmental switch in choanoflagellates. Proc. Natl. Acad. Sci. USA 113, 7894–7899. https://doi.org/10.1073/pnas.1605015113.
Wurl, O., Wurl, E., Miller, L., Johnson, K., Vagle, S., 2011. Formation and global distribution of sea-surface microlayers. Biogeosciences 8, 121–135. https://doi.org/10.5194/bg-8-121-2011.
Wurl, O., Stolle, C., Van Thuoc, C., The Thu, P., Mari, X., 2016. Biofilm-like properties of the sea surface and predicted effects on air–sea CO2 exchange. Prog. Oceanogr. 144, 15–24. https://doi.org/10.1016/j.pocean.2016.03.002.
Xian, F., Hendrickson, C.L., Blakney, G.T., Beu, S.C., Marshall, A.G., 2010. Automated broadband phase correction of Fourier transform ion cyclotron resonance mass spectra. Anal. Chem. 82, 8807–8812. https://doi.org/10.1021/ac101091w.
Zäncker, B., Bracher, A., Röttgers, R., Engel, A., 2017. Variations of the organic matter composition in the sea surface microlayer: a comparison between Open Ocean, coastal, and upwelling sites off the Peruvian coast. Front. Microbiol. 8, 2369. https://doi.org/10.3389/fmicb.2017.02369.
Zhang, T., Marchant, R.E., 1996. Novel polysaccharide surfactants: The effect of hydrophobic and hydrophilic chain length on surface active properties. J. Colloid Interface Sci. 177, 419–426. https://doi.org/10.1006/jcis.1996.0054.
Zhang, X., Li, Y., Cui, Z., Gu, M., Zang, X., Li, Y., Chen, X., Sun, X., Xu, N., 2024. Light intensity influences the glycerolipid remodeling of *Gracilariopsis lemaneiformis* in response to short-term high temperature stress. Aquaculture 583, 740566. https://doi.org/10.1016/j.aquaculture.2024.740566.